DUOXA1-mediated ROS production promotes cisplatin resistance by activating ATR-Chk1 pathway in ovarian cancer

Yunxiao Meng[1,2,11], Chi-Wei Chen[1,2,11], Mingo MH Yung[3], Wei Sun[4], Jing Sun[1,2], Zhuqing Li[1,2], Jing Li[1,2], Zongzhu Li[1,2], Wei Zhou[1,2,5], Stephanie S Liu[3], Annie NY Cheung[6], Hextan YS Ngan[3], John C. Braisted[4], Yan Kai[2,7], Weiqun Peng[7], Alexandros Tzatsos[2,8], Yiliang Li[9], Zhijun Dai[10], Wei Zheng[4,*], David W. Chan[3,*], Wenge Zhu[1,2,*]

[1]Department of Biochemistry and Molecular Medicine, The George Washington University School of Medicine and Health Sciences, Washington, DC 20037, USA.
[2]GW Cancer Center, The George Washington University, Washington, DC 20052, USA.
[3]Department of Obstetrics and Gynecology, LKS Faculty of Medicine, The University of Hong Kong, Hong Kong SAR, China.
[4]National Center for Advancing Translational Sciences, National Institutes of Health, Bethesda, MD 20892, USA.
[5]Department of Colorectal Surgery, Sir Run Run Shaw Hospital, School of Medicine, Zhejiang University, Hangzhou 310016, China.
[6]Department of Pathology, LKS Faculty of Medicine, The University of Hong Kong, Hong Kong SAR, China.
[7]Department of Physics, The George Washington University Columbian College of Arts & Sciences, Washington, DC 20052, USA.
[8]Department of Anatomy and Regenerative Biology, The George Washington University School of Medicine and Health Sciences, Washington, DC 20037, USA.
[9] Tianjin Key Laboratory of Radiation Medicine and Molecular Nuclear Medicine, Institute of Radiation Medicine, Peking Union Medical College & Chinese Academy of Medical Sciences, Tianjin 300192, China.
[10]Department of Oncology, the Second Affiliated Hospital, Xi'an Jiaotong University, Xi'an 710004, China.
[11]Co-first authors.
* Co-corresponding authors:

David W Chan, Tel: (852) 39179367; Email: dwchan@hku.hk

Wei Zheng, Tel: 301-217-5251; Email: wzheng@mail.nih.gov

Wenge Zhu, Tel: 202-994-3125; Email: wz6812@gwu.edu

Running Title: DUOXA1 regulates cisplatin resistance

Abstract

The acquisition of resistance is a major obstacle to the clinical use of platinum drugs for ovarian cancer treatment. Increase of DNA damage response is one of major mechanisms contributing to platinum-resistance. However, how DNA damage response is regulated in platinum-resistant ovarian cancer cells remains unclear. Using quantitative high throughput combinational screen (qHTCS) and RNA-sequencing (RNA-seq), we show that dual oxidase maturation factor 1 (DUOXA1) is overexpressed in platinum-resistant ovarian cancer cells, resulting in over production of reactive oxygen species (ROS). Elevated ROS level sustains the activation of ATR-Chk1 pathway, leading to resistance to cisplatin in ovarian cancer cells. Moreover, using qHTCS we identified two Chk1 inhibitors (PF-477736 and AZD7762) that re-sensitize resistant cells to cisplatin. Blocking this novel pathway by inhibiting ROS, DUOXA1, ATR or Chk1 effectively overcomes cisplatin resistance *in vitro* and *in vivo*. Significantly, the clinical studies also confirm the activation of ATR and DOUXA1 in ovarian cancer patients, and elevated DOUXA1 or ATR-Chk1 pathway correlates with poor prognosis. Taken together, our findings not only reveal a novel mechanism regulating cisplatin resistance, but also provide multiple combinational strategies to overcome platinum-resistance in ovarian cancer.

Keywords: ROS; high throughput screen, cisplatin resistance; ovarian cancer; DUOXA1; ATR-Chk1

Abbreviations: qHTCS, quantitative high throughput combinational screen; RNA-seq, RNA-sequencing; DUOXA1, dual oxidase maturation factor 1; ROS, reactive oxygen species

Highlights:

- Providing multiple potential approaches for treatment of platinum resistant ovarian cancer
- Integrating qHTCS, RNA-seq and clinical studies to elucidate cisplatin resistant mechanism
- DUOXA1-mediated activation of ATR-Chk1 regulates cisplatin resistance in ovarian cancer

1. Introduction

Accumulating evidence has showed that most of advanced ovarian cancer patients have a good response to initial therapy with combination of cytoreductive surgery and platinum-based chemotherapy [1]. However, approximately 70% of patients will develop resistance to platinum drugs over the time of treatment [2, 3]. Multiple mechanisms have been identified to regulate platinum-resistance [4]. Among them, increased DNA damage response is positively correlated with platinum-resistance [5-7]. However, the mechanism of sustaining the high activity of DNA damage response in platinum resistant ovarian cancer cells remains largely unknown.

Reactive oxygen species (ROS) is composed of free radicals and reactive metabolites, such as superoxide, hydroxyl radical, and hydroxide [8]. Emerging evidence has shown that ROS act as a double-edged sword in living organisms [9]. Low dose of ROS is able to promote cell proliferation, mediate cell signal transduction, and under certain circumstance can promote cellular survival and tumor growth [10-12]. In contrast, excessive amount of ROS is capable of causing cellular damage on lipid, DNA, RNA and proteins [13]. In cancer cells, increased ROS accumulation can be resulted from activation of oncogenes [14-16]. Several proteins are well-known in regulating ROS production, including FOXM1, DPP4, PTPN11, ABL1, and Dual oxidase 1 (DUOX1) [15-19]. Dual oxidase 1 (DUOX1) is composed of DUOXA1 and DUOXA2 [20, 21]. DUOX1 has been shown to mediate thyroid hormonogenesis through production of hydrogen peroxide [22]. It was also reported that overexpression of DUOXA1 inhibits murine muscle satellite cell differentiation by raising ROS production [19].

It is well documented that platinum drugs kill cancer cells by introducing DNA crosslinks via covalent bond between DNA bases and thereby, reducing cell viability [23]. FANCD2 and other members of Fanconi anemia family play a critical role in repairing DNA crosslink damage. Activation of FANCD2 is regulated through its mono-ubiquitination [24-27]. ATR (ataxia telangiectasia and Rad3-related protein) is a serine/threonine protein kinase that is essential to regulate DNA damage response in cells with DNA crosslinks [28]. In cells with DNA crosslinks, ATR activates Checkpoint kinase 1 (Chk1) by phosphorylation of at Ser-317 and Ser-345 [29].

Chk1 is important to mediate DNA damage repair by activating repair factors such as Rad51, FANCE and PCNA [30].

To identify the novel mechanism regulating cisplatin resistance, we conducted a quantitative high throughput combinational screen (qHTCS) together with RNA-sequencing (RNA-seq) in cisplatin resistant ovarian cancer cells [31, 32]. From this qHTCS, we identified two Chk1 inhibitors (PF-477736 and AZD7762) that synergistically enhanced cisplatin efficacy against cisplatin resistant ovarian cancer cells. Significantly, we found DOUXA1 was up-regulated in platinum-resistant cells and elevated DOUXA1 increased ROS levels, which sustained the active ATR-Chk1 pathway. Inhibition of ROS, DUOXA1, ATR or Chk1 effectively overcame cisplatin resistance *in vitro* or *in vivo*. The clinical studies also confirmed the activation of ATR and DUOXA1 in recurrent and resistant ovarian cancer patients, and elevated ATR-Chk1 or DOUXA1 was correlated with poor prognosis in ovarian cancer patients who have received platinum drug-based therapy.

2. Methods and Materials

2.1. Cell lines and generation of resistant cells SKOV3 was from the American Type Culture Collection (ATCC). PEO14 and PEO23 were from Sigma-Aldrich. SKOV3 was cultured in Dulbecco's Modified Eagle's medium supplemented with 10% fetal bovine serum (FBS). PEO14 and PEO23 were cultured in RPMI-1640 supplemented with 10% FBS. Establishment of cisplatin resistant cell line SKOV3 CR was as described previously [33]. Details were provided in Appendix S1 (Supplementary methods).

2.2. Antibodies and reagents were provided in Appendix S1 (Supplementary methods)

2.3. Cell viability assay Cell viability and IC_{50} were measured as previous descriptions [34] [35]. Details were provided in Appendix S1 (Supplementary methods).

2.4. Quantitative high throughput combinational screen (qHTCS) Assay was followed as the previous study [32]. Details were provided in Appendix S1 (Supplementary methods).

2.5. **RNA-sequencing (RNA-seq)** Cells were collected at log growth phase. RNA isolation and RNA sequencing were performed by Q2 Solutions – EA Genomics. RNA sequence data have been submitted to Gene Expression Omnibus (GEO). The accession number is GSE98559. Details were provided in Appendix S1 (Supplementary methods).

2.6. **Kaplan-Meier plotter** Patients survival rates were analyzed with GSE and TCGA databases using platform (http://kmplot.com). Details were provided in Appendix S1 (Supplementary methods) [36].

2.7. **Specimens of ovarian cancer patients** Detailed information on human subject was provided in Appendix S1 (Supplementary methods) and Appendix S2 (Supplementary table).

2.8. **Immunohistochemistry** Details were provided in Appendix S1 (Supplementary methods).

2.9. **siRNA interference** siRNA targeting Chk1 , DUOXA1, and a negative control (siGL2) were as described previously [37-39]. Details were provided in Appendix S1 (Supplementary methods).

2.10. **Flow cytometry and Modified comet assay** Assays were performed as previous study [40]. Details were provided in Appendix S1 (Supplementary methods).

2.11. **Clonogenic cell survival assay and Metaphase chromosome spread** Details were provided in Appendix S1 (Supplementary methods).

2.12. **Reactive Oxygen Species (ROS) detection, qPCR, and TUNEL assay** Details were provided in Appendix S1 (Supplementary methods).

2.13. **Animal experiments** Animal housing and all procedures were conducted with protocols approved by the Institutional Animal Care and Use Committees (IACUC) of The George Washington University. Details were provided in Appendix S1 (Supplementary methods).

3. Results

3.1. qHTCS and RNA-seq to identify Chk1 inhibitors that overcome cisplatin resistance in ovarian cancer cells

The main goal of this study is to integrate two platforms, qHTCS and genomic sequencing, to identify novel mechanisms regulating platinum-resistance in ovarian cancer and small molecules that can overcome platinum resistance in ovarian cancer cells. The identified pathways will be further confirmed by *in vivo* as well as clinical studies (Figure 1A). We first generated the cisplatin resistant cells using procedures as described previously and in methods [41, 42]. A resistant cell line, SKOV3 CR, was generated that exhibited 5-fold increase of IC_{50} to cisplatin compared to sensitive SKOV3 cells (Figure 1B). To further confirm the pathway identified in the resistant cells generated in cell culture dish, we obtained another pair of platinum-sensitive and -resistant ovarian cancer cells, PEO14 and PEO23, which were derived directly from the same patient before and after development of platinum drug resistance [42]. Clearly, PEO23 exhibited a 4-fold increase of IC_{50} to cisplatin compared to its sensitive counterpart PEO14 (Figure 1B).

We next conducted a qHTCS using SKOV3 CR cells to identify compounds that can re-sensitize SKOV3 CR cells to cisplatin. To accomplish this goal, we performed a two-round screening. In the first-round screening with a total of 6,016 compounds from libraries of NPC (NCGC Pharmaceutical Collection), MIPE (Mechanism Interrogation Plate) and LOPAC (The Library of Pharmacologically Active Compounds), we identified 112 compounds that exhibited strong killing efficacy against resistant cells. To further discover compounds that have synergy with cisplatin, these 112 compounds were screened at 11 different concentrations in combination with cisplatin at 20 μM. The second-round screening identified two Chk1 inhibitors, PF-477736 and AZD7762 [43, 44], which re-sensitized resistant cells to cisplatin (Figure 1C). PF-477736 and AZD7762 are on clinical trials for treating advanced solid tumors in combined with gemcitabine or irinotecan [45, 46]. These results suggest that activation of Chk1 pathway may play an important role in the regulation of cisplatin resistance in ovarian cancer cells.

3.2. Clinical evidence that ATR-Chk1 is activated in tumors from platinum drug recurrent or resistant patients

To explore the clinical relevance of Chk1 activation in the regulation of platinum drug resistance in ovarian cancer, we conducted RNA-Seq analyses to examine the gene expression profiles of SKOV3 and SKOV3 CR cells. A total of 3414 genes were found to be upregulated at least 1.5 folds in resistant cells. We next examined the correlation of Chk1 activation with the survival of ovarian cancer patients who have received platinum drug-based therapy. Since Chk1 is activated by its phosphorylation, we therefore investigated the correlation of patient survival with gene expression levels of Chk1 functional related genes. Specifically, using PathwayNet analysis (http://pathwaynet.princeton.edu), we identified a total of 392 genes that are functionally linked to Chk1 (Figure 1D). Comparing these genes with up-regulated genes identified by RNA-Seq, we identified a total of 108 genes linked to Chk1 function and were up-regulated in SKOV3 CR cells (Figure 1D). We named these genes as ATR-Chk1 signature genes. KEGG (http://www.genome.jp/kegg/pathway.html) pathway analyses indicated that these genes regulate cell-cycle, DNA replication, DNA repair, etc. (Figure 1E).

Since inhibition of Chk1 activity re-sensitized resistant cells to cisplatin, we hypothesized that the expression levels of ATR-Chk1 signature genes may be negatively correlated with survival of ovarian cancer patients. To test this hypothesis, we analyzed the data from ~500 ovarian cancer patients from TCGA database and compared expression levels of ATR-Chk1 signature genes with survival rate of these patients using Kaplan-Meier plotter [36]. Significantly, patients carrying higher expression levels of ATR-Chk1 signature genes displayed a poor overall survival rate and progression free survival rate (PFS) (Figure 1F).

The best way to evaluate the correlation of the ATR-Chk1 pathway with platinum-resistance in ovarian cancer is to examine and compare the activation of ATR-Chk1 in the tumor samples from the same patient before platinum drug treatment and after development of tumor recurrence or resistance. To this end, we identified a total of seven patients who have received platinum drug-based chemotherapy and had a recurrence or resistance 11-41 months post treatment. Immunohistochemistry (IHC) results indicated that the levels of phosphorylation of ATR at Thr-1989 (pATR) were increased in four out of seven recurrent tumor samples (Figure 1G, Supplementary table S1), suggesting that the upregulated ATR-Chk1

pathway is an important mechanism contributing to cisplatin resistance of ovarian cancer. Significantly, one patient (Patient 1) has been confirmed clinically as a platinum-resistant ovarian cancer patient and the IHC analysis indicated that pATR levels were significantly increased in resistant tumors compared to sensitive tumor (Figure 1H).

3.3. Chk1 inhibition synergizes with cisplatin in cisplatin resistant ovarian cancer cells

Encouraged by the above clinical discovery, we examined whether inhibition of Chk1 by PF-477736 or AZD7762 has synergistic effects with cisplatin in cisplatin resistant ovarian cancer cells. To this end, we first measured the cell proliferation and the synergistic effect between PF-477736 or AZD7762 and cisplatin using SRB cytotoxicity assay. The combination index (CI) was employed to measure effects of the interaction between two drugs (synergism: CI < 1; additive effect: CI = 1; and antagonism: CI > 1) [35]. Combined PF-477736 with cisplatin exhibited a good synergistic effect (CI < 1) on suppressing growth of SKOV3 CR cells (Figure 2A). AZD7762 in the combination with cisplatin also displayed a good synergistic effect in SKOV3 CR cells at several combination windows (Figure 2B). Significantly, the combination of PF-477736 or AZD7762 with cisplatin exhibited very good synergistic effects in PEO23 cells derived directly from the platinum resistant ovarian patient (Figure 2C-D).

To rule out the off-target effects of Chk1 inhibitors, we next examined whether knockdown of Chk1 by siRNA could re-sensitize resistant cells to cisplatin. We observed that Chk1 inhibition by siChk1 significantly reduced IC_{50} to cisplatin in resistant cells compared to siGl2 control treated cells (from 24.14 μM to 3.59 μM; Figure 2E). The apoptotic analysis indicated that Chk1 inhibition significantly increased apoptotic cell death of resistant cells with cisplatin treatment (Figure 2F). Thus, Chk1 activation is critical to regulate cisplatin resistance in ovarian cancer cells.

3.4. ATR-Chk1 pathway is activated in resistant ovarian cancer cells

To elucidate the molecular mechanism of platinum-resistance in ovarian cancer cells, we examined the activation of ATR-Chk1 pathway in sensitive and resistant cells. Strikingly, phosphorylations of Chk1 at Ser-317 and ATR at Thr-1989 were increased in both cisplatin-

resistant SKOV3 CR and PE023 cells (Figure 3A), indicating that the ATR-Chk1 pathway was activated. Interestingly, FANCD2 protein level was also increased in both resistant cell lines (Figure 3A).

We next examined whether inhibition of ATR has synergistic effects with cisplatin in resistant cells. To this goal, we used ATR inhibitor (VE-821) to treat SKOV3 CR cells together with cisplatin and found that VE-821 re-sensitized SKOV3 CR cells to cisplatin (Figure 3B). Consistently, the combination of cisplatin with VE-821 exhibited a good synergistic effect in both SKOV3 CR and PEO23 cells (Figure 3C-D). Importantly, VE-821 indeed reduced the activation of both ATR and Chk1 (Figure 3E), and increased apoptosis as indicated by FACS and cleaved PARP-1 in SKOV3 CR cells (Figure 3F).

3.5. G2/M phase checkpoint is activated in cisplatin resistant ovarian cancer cells

We noticed that resistant SKOV3 CR and PEO23 cells grew slowly compared to their sensitive counterparts SKOV3 and PEO14 cells. Given that ATR-Chk1 pathway was activated in SKOV3 CR and PEO23 cells, we assumed that activated DNA damage response may interfere with cell-cycle progression. To test this hypothesis, we measured and compared the cell cycle progression of sensitive and resistance cells by FACS. Interestingly, compared to sensitive cell SKOV3, SKOV3 CR cells exhibited a G2/M phase accumulation (22% in SKOV3 cells and 33% in SKOV3 CR cells) (Figure 4A). Increased G2/M phase cell population indicates that G2/M phase checkpoint may be activated. Indeed, we detected the increased phosphorylation of Cdc2 at Tyr-15 (pCdc2), a marker of activation of G2/M phase checkpoint, in SKOV3 CR cells (Figure 4B). Activation of G2/M phase checkpoint prevents cells from entering mitosis [47]. We therefore examined the phosphorylation of H3 at Ser-10 (pH3), which is mitotic marker, and found a decreased phosphorylation of H3 at Ser10 in SKOV3 CR cells (Figure 4B), indicating an accumulation of cells at G2 phase before entering mitosis.

Up-regulated ATR-Chk1 pathway in platinum-resistant ovarian cancer cells suggests a higher DNA damage repair activity. To test this possibility, we measured and compared the DNA damage repair capability in both platinum-sensitive and -resistant cells. Using metaphase

chromatin spread assay to examine the DNA breakage, we found that there was no difference of DNA breakage between SKOV3 and SKOV3 CR cells in DMSO treated cells (Figure 4C). However, cisplatin treatment significantly increased the percentage of breakage in SKOV3 cells compared to SKOV3 CR cells (35% in SKOV3 cells and 15% in SKOV3 CR cells) (Figure 4C). Micronucleus is the small nucleus that forms whenever a chromosome or a fragment of a chromosome is not incorporated into one of the daughter nuclei during cell division and usually is regarded as a sign of genotoxic events and chromosomal instability [48]. Interestingly, Aphidicolin induced more micronuclei in SKOV3 cells (18%) than in SKOV3 CR cells (11%) (Figure 4D). Taken together, our data indicates that G2/M checkpoint is activated in resistant cells.

3.6. Elevated DNA damage repair activity in resistant ovarian cancer cells

To rule out the possibility that the acquired resistance of SKOV3 CR cells was due to reduced cisplatin uptaking, we measured the DNA interstrand crosslinks (ICLs) in both sensitive end resistant cells after cisplatin treatment using a modified comet assay [49]. This assay is used to quantify amount DNA ICLs by the intensity of comet-like images (named as tail moment). After 2-hour incubation of cisplatin, cells received radiation of 20 Gy to shear DNA fragment randomly before analyzed with modified comet assay. As shown in Figure 5A, there was no difference in the amount of ICLs between SKOV3 and SKOV3 CR cells, indicating that failure to uptake cisplatin in resistant cells is not the case. Given that ATP7A and ATP7B are known for effluxion of cisplatin in cells [50, 51], we further measure the protein levels in SKOV3 and SKOV3 CR cells, and found the similar expression levels of ATP7A and ATP7B in both cells, suggesting that the resistance in SKOV3 CR cells is not due to the abnormal drug effluxion effect (Figure 5B).

We next examined the DNA repair activity using the modified comet assay. Cells were treated with cisplatin and then released into cisplatin-free medium. We first measured the lengths of tail movements and found that the reduction of tail movements in SKOV3 CR was faster than SKOV3 cells (Figure 5C), indicating that SKOV3 CR cells have stronger ability to remove DNA ICLs induced by cisplatin. FANCD2 plays a critical role in the repair of ICLs [24-27]. We next examined the activation of FANCD2 by measuring ubiquitination of FANCD2 levels in

cells after cisplatin treatment. Strikingly, the ubiquitination of FANCD2 in SKOV3 CR cells decreased faster than that in SKOV3 cells (Figure 5D-E), indicating a stronger DNA repair activity in SKOV3 CR cells. Consistently, SKOV3 CR cells exhibited less Chk1 phosphorylation at Ser-317 compared to sensitive cells (Figure 5F-G).

3.7. DUOXA1-mediated-ROS production sustains the elevated DNA damage response in resistant ovarian cancer cells

The next question is how ovarian cancer cells sustain the activated DNA damage response in platinum-resistant ovarian cancer cells. Since cisplatin can increase ROS levels [52], we hypothesized that after a long-term cisplatin treatment, the platinum-resistant ovarian cells may acquire a mechanism to sustain higher levels of ROS to activate DNA damage response. To test this hypothesis, we first examined ROS level and found that ROS level in both SKOV3 CR and PEO23 cells were increased compared to their sensitive counterparts SKOV3 and PEO14 cells (Figure 6A). To test whether ROS is a driving force for activating DNA damage response in resistant ovarian cells, we inhibited ROS production by using a ROS inhibitor called YCG063 [53]. Notably, YCG063 reduced ROS level in both SKOV3 CR and PEO23 cells (Figure 6B) and inhibition of ROS by YCG063 reduced levels of pATR, pChk1 and γH2AX in both platinum-resistant ovarian cells (Figure 6C). Consistent with above results, inhibition of ROS by ROS inhibitors YCG063 or MnTmpyp decreased pCdc2 level and increased pH3 level (Figure 6D), indicating that inhibition of ROS production abolishes G2/M checkpoint.

To investigate the mechanism of how ROS level is up-regulated, we analyzed the ROS related gene expression in SKOV3 CR cells from RNA-seq results and identified a total of 11 ROS related genes that were up-regulated in SKOV3 CR cells compared to SKOV3 cells (Figure 6E). Of these genes, DUOXA1 draw our attention because it has been reported to be critical in the regulation of ROS and up-regulation of DUOXA1 can promote ROS level [19]. qPCR and western blotting analyses indicated that DUOXA1 was overexpressed in SKOV3 CR and PEO23 cells at both mRNA and protein levels (Figure 6F-G).

To clarify the role of DUOXA1 in the regulation of cisplatin resistance, we depleted DUOXA1 by siRNA and found that downregulation of DUOXA1 reduced ROS levels (Figure 6H). Significantly, depletion of DUOXA1 decreased the phosphorylation of ATR and Chk1 and re-sensitized SKOV3 CR cells to cisplatin (Figure 6I-J). Consistently, depletion of DUOXA1 increased the apoptotic population in SKOV3 CR cells when treated with cisplatin (Fig. 6K). We next examined whether expression level of DUOXA1 correlates with poor survival of ovarian cancer patients with platinum treatment history. As expected, ovarian cancer patients carrying higher expression levels of DUOXA1 exhibited a poor overall survival rate (Figure 6L). To evaluate the whether DUOXA1 is up-regulated in tumor samples from resistant ovarian cancer patients, we examined the expression levels of DUOXA1 protein in tumor samples from the same patients before and after development of platinum drug resistance by IHC. Significantly, DUOXA1 levels were increased in six of seven patients (Figure 6M and Supplemental Figure 2D).

3.8. ATR inhibition suppresses SKOV3 CR xenograft tumor growth

We tested whether inhibition of ATR-Chk1 pathway by using an ATR specific inhibitor VE-822 could suppress SKOV3 CR tumor growth in mice [54]. To this end, we first subcutaneously implanted SKOV3 CR xenograft tumors in nude mice and then administrated VE-822 to the animals. While SKOV3 CR tumors were resistant to cisplatin or VE-822 treatment, the combinatorial treatment of cisplatin with VE-822 significantly repressed tumors growth (Figure 7A). To evaluate effect and toxicity of VE-822 and cisplatin treatment, we collected tissues from xenograft tumors, livers, and kidney. Immunohistochemistry (IHC) analysis showed that VE-822 plus cisplatin did not cause obvious histopathological alterations, lesions of hepatotoxicity, and kidney toxicity (Figure 7B). Significantly, VE-822 treatment alone or in combined with cisplatin efficiently reduced the phosphorylation of ATR in tumors (Figure 7C). The combination of VE-822 with cisplatin induced the apoptosis in tumors as indicated by a positive TUNEL staining (Figure 7D).

4. Discussion

In this study, we used an unbiased qHTCS assay to identify Chk1 inhibitors that re-sensitize cisplatin resistant ovarian cancer cells to cisplatin. Subsequent analyses identified elevated DUOXA1 as a driving force for activating and sustaining high level of ROS, which promotes cisplatin resistance by activating ATR-Chk1 pathway (Figure 7E). Importantly, we provided the clinical evidence showing that activated ATR and DUOXA1 are found in platinum-resistant tumor tissues of ovarian cancer patients and the elevated ATR-Chk1 pathway and DUOXA1 is correlated with poor survival of ovarian cancer patients who have received platinum-based therapeutic treatments. Although the activated ATR-Chk1 in the regulation of cisplatin-resistance has been reported [55, 56], the molecular mechanism of how platinum-resistant ovarian cancer cells sustain activated ATR-Chk1 is unknown. Therefore, our study provides with a new mechanistic insight of how ovarian cancer cells develop cisplatin-resistance over the time of treatment. This regulatory can be used as an intervention point for treatment of drug resistant ovarian cancer in future.

Using qHTCS, we identified two Chk-1 inhibitors, PF-477736 and AZD7762, which synergistically suppress cisplatin-resistant ovarian cancer cells with cisplatin. A clinical trial at phase I (NCT00437203) has been conducted for determining the maximum tolerated dose of PF-477736 in the combination with gemcitabine in patients with advanced solid malignancies. AZD7762 showed its therapeutic potential in several clinical trials when combined with gemcitabine or Irinotecan [45, 46]. In our study, we demonstrated that the combination of two Chk1 inhibitors with cisplatin led to a promising and efficient treatment for cisplatin resistant ovarian cancer cells. Therefore, the combinational therapy of Chk1 inhibitors with platinum drugs is warranted for clinical trials to treat the cisplatin resistant ovarian cancer patients to evaluate the efficacy and safety.

It is exciting to find that ROS level is elevated in resistant ovarian cancer cells and increased ROS by overexpression of DUOXA1 sustains the activation of ATR-Chk1 signaling. To our knowledge, this is the first evidence to link DUOXA1-mediated ROS to ATR-Chk1 in the regulation of platinum-resistance. While it is reported that the ROS signaling can stimulate cell survival factors [11], our study has revealed a novel alternative role of ROS signaling that

promotes DNA damage response, resulting in cisplatin resistance. Although DUOXA1 is known to enhance ROS level by producing hydrogen peroxide [22], the detail mechanism of how DUOXA1 level is regulated in cisplatin resistant ovarian cancer cells is still unknown.

Over decades, platinum drugs are widely used as single or in combined with other anticancer agents to treat various types of cancers, such as lung cancer, color cancer, bladder cancer, head and neck cancer, ovarian cancer, and testicular cancers [57]. Therefore, targeting the DUOXA1-ROS-ATR-Chk1 signaling cascade would be a potential therapeutic approach for treatment of other platinum-resistant cancers that may have developed the same resistant mechanism.

Author contributions

Y.M., C.C., W.S., W. Zheng, D.W.C., W. Zhu contributed to design experiments, interpret results, and write the manuscript. Y.M., C.C., W.S., W. Zhou, J.L., J.S., Zhuqing Li, Zongzhu Li., J.C.B., Y.K., W.P., A.T., Y.L., Z.D., contributed to perform experiments. M.M.Y., S.S.L., A.N.C., H.Y.N., D.W.C., contributed to collection and analyze the samples from patients. W. Zheng and W. Zhu supervised the project and acquired funding. All authors assisted in editing the manuscript and approved it before submission.

Conflicts of Interest

None to declare

Acknowledgements

This work was partially supported by funding from the National Institutes of Health (CA177898 and CA184717 to W. Zhu), the McCormick Genomic and Proteomic Center, and intramural research program at the National Center for Advancing Translational Sciences (NCATS). W. Zhu

was supported by a Research Scholar Grant, RSG-13-214-01-DMC from the American Cancer Society.

Reference

1. M. Petrillo, L.P. Anchora, G. Scambia, and A. Fagotti, *Cytoreductive Surgery Plus Platinum-Based Hyperthermic Intraperitoneal Chemotherapy in Epithelial Ovarian Cancer: A Promising Integrated Approach to Improve Locoregional Control.* Oncologist, 2016. **21**(5): p. 532-4.
2. L.C. Hanker, S. Loibl, N. Burchardi, J. Pfisterer, W. Meier, E. Pujade-Lauraine, I. Ray-Coquard, J. Sehouli, P. Harter, and A. du Bois, *The impact of second to sixth line therapy on survival of relapsed ovarian cancer after primary taxane/platinum-based therapy.* Ann Oncol, 2012. **23**(10): p. 2605-12.
3. L. Galluzzi, I. Vitale, J. Michels, C. Brenner, G. Szabadkai, A. Harel-Bellan, M. Castedo, and G. Kroemer, *Systems biology of cisplatin resistance: past, present and future.* Cell Death Dis, 2014. **5**: p. e1257.
4. L. Galluzzi, L. Senovilla, I. Vitale, J. Michels, I. Martins, O. Kepp, M. Castedo, and G. Kroemer, *Molecular mechanisms of cisplatin resistance.* Oncogene, 2012. **31**(15): p. 1869-83.
5. L.P. Martin, T.C. Hamilton, and R.J. Schilder, *Platinum resistance: the role of DNA repair pathways.* Clin Cancer Res, 2008. **14**(5): p. 1291-5.
6. P.A. Vasey, *Resistance to chemotherapy in advanced ovarian cancer: mechanisms and current strategies.* Br J Cancer, 2003. **89 Suppl 3**: p. S23-8.
7. R. Agarwal and S.B. Kaye, *Ovarian cancer: strategies for overcoming resistance to chemotherapy.* Nat Rev Cancer, 2003. **3**(7): p. 502-16.
8. H. Sies, *Oxidative stress: oxidants and antioxidants.* Exp Physiol, 1997. **82**(2): p. 291-5.
9. K.R. Martin and J.C. Barrett, *Reactive oxygen species as double-edged swords in cellular processes: low-dose cell signaling versus high-dose toxicity.* Hum Exp Toxicol, 2002. **21**(2): p. 71-5.
10. D. Samanta, D.M. Gilkes, P. Chaturvedi, L. Xiang, and G.L. Semenza, *Hypoxia-inducible factors are required for chemotherapy resistance of breast cancer stem cells.* Proc Natl Acad Sci U S A, 2014. **111**(50): p. E5429-38.
11. D. Trachootham, J. Alexandre, and P. Huang, *Targeting cancer cells by ROS-mediated mechanisms: a radical therapeutic approach?* Nat Rev Drug Discov, 2009. **8**(7): p. 579-91.
12. J.P. Fruehauf and F.L. Meyskens, Jr., *Reactive oxygen species: a breath of life or death?* Clinical Cancer Research, 2007. **13**(3): p. 789-94.
13. P.T. Schumacker, *Reactive oxygen species in cancer: a dance with the devil.* Cancer Cell, 2015. **27**(2): p. 156-7.
14. K. Irani, *Oxidant signaling in vascular cell growth, death, and survival : a review of the roles of reactive oxygen species in smooth muscle and endothelial cell mitogenic and apoptotic signaling.* Circ Res, 2000. **87**(3): p. 179-83.
15. M. Sattler, S. Verma, G. Shrikhande, C.H. Byrne, Y.B. Pride, T. Winkler, E.A. Greenfield, R. Salgia, and J.D. Griffin, *The BCR/ABL tyrosine kinase induces production of reactive oxygen species in hematopoietic cells.* J Biol Chem, 2000. **275**(32): p. 24273-8.

16. H.J. Park, J.R. Carr, Z. Wang, V. Nogueira, N. Hay, A.L. Tyner, L.F. Lau, R.H. Costa, and P. Raychaudhuri, *FoxM1, a critical regulator of oxidative stress during oncogenesis.* EMBO J, 2009. **28**(19): p. 2908-18.
17. A.P. Femia, L. Raimondi, G. Maglieri, M. Lodovici, E. Mannucci, and G. Caderni, *Long-term treatment with Sitagliptin, a dipeptidyl peptidase-4 inhibitor, reduces colon carcinogenesis and reactive oxygen species in 1,2-dimethylhydrazine-induced rats.* International Journal of Cancer, 2013. **133**(10): p. 2498-503.
18. D. Xu, H. Zheng, W.M. Yu, and C.K. Qu, *Activating mutations in protein tyrosine phosphatase Ptpn11 (Shp2) enhance reactive oxygen species production that contributes to myeloproliferative disorder.* PLoS One, 2013. **8**(5): p. e63152.
19. S.D. Sandiford, K.A. Kennedy, X. Xie, J.G. Pickering, and S.S. Li, *Dual oxidase maturation factor 1 (DUOXA1) overexpression increases reactive oxygen species production and inhibits murine muscle satellite cell differentiation.* Cell Commun Signal, 2014. **12**: p. 5.
20. S. Luxen, D. Noack, M. Frausto, S. Davanture, B.E. Torbett, and U.G. Knaus, *Heterodimerization controls localization of Duox-DuoxA NADPH oxidases in airway cells.* J Cell Sci, 2009. **122**(Pt 8): p. 1238-47.
21. S. Morand, T. Ueyama, S. Tsujibe, N. Saito, A. Korzeniowska, and T.L. Leto, *Duox maturation factors form cell surface complexes with Duox affecting the specificity of reactive oxygen species generation.* FASEB J, 2009. **23**(4): p. 1205-18.
22. H. Ohye and M. Sugawara, *Dual oxidase, hydrogen peroxide and thyroid diseases.* Exp Biol Med (Maywood), 2010. **235**(4): p. 424-33.
23. S. Dasari and P.B. Tchounwou, *Cisplatin in cancer therapy: molecular mechanisms of action.* Eur J Pharmacol, 2014. **740**: p. 364-78.
24. A.D. D'Andrea and M. Grompe, *The Fanconi anaemia/BRCA pathway.* Nat Rev Cancer, 2003. **3**(1): p. 23-34.
25. U. Jo and H. Kim, *Exploiting the Fanconi Anemia Pathway for Targeted Anti-Cancer Therapy.* Mol Cells, 2015. **38**(8): p. 669-76.
26. C.C. Liang, Z. Li, D. Lopez-Martinez, W.V. Nicholson, C. Venien-Bryan, and M.A. Cohn, *The FANCD2-FANCI complex is recruited to DNA interstrand crosslinks before monoubiquitination of FANCD2.* Nat Commun, 2016. **7**: p. 12124.
27. C. Lachaud, A. Moreno, F. Marchesi, R. Toth, J.J. Blow, and J. Rouse, *Ubiquitinated Fancd2 recruits Fan1 to stalled replication forks to prevent genome instability.* Science, 2016. **351**(6275): p. 846-9.
28. P. Pichierri and F. Rosselli, *The DNA crosslink-induced S-phase checkpoint depends on ATR-CHK1 and ATR-NBS1-FANCD2 pathways.* EMBO J, 2004. **23**(5): p. 1178-87.
29. R.L. Flynn and L. Zou, *ATR: a master conductor of cellular responses to DNA replication stress.* Trends Biochem Sci, 2011. **36**(3): p. 133-40.
30. Y.W. Zhang and T. Hunter, *Roles of Chk1 in cell biology and cancer therapy.* International Journal of Cancer, 2014. **134**(5): p. 1013-1023.
31. C.Y. Lee, R.L. Johnson, J. Wichterman-Kouznetsova, R. Guha, M. Ferrer, P. Tuzmen, S.E. Martin, W. Zhu, and M.L. DePamphilis, *High-throughput screening for genes that prevent excess DNA replication in human cells and for molecules that inhibit them.* Methods, 2012. **57**(2): p. 234-48.
32. W. Sun, R.A. Weingarten, M. Xu, N. Southall, S. Dai, P. Shinn, P.E. Sanderson, P.R. Williamson, K.M. Frank, and W. Zheng, *Rapid antimicrobial susceptibility test for identification of new therapeutics and drug combinations against multidrug-resistant bacteria.* Emerg Microbes Infect, 2016. **5**(11): p. e116.

33. A.A. Jazaeri, E. Shibata, J. Park, J.L. Bryant, M.R. Conaway, S.C. Modesitt, P.G. Smith, M.A. Milhollen, A.J. Berger, and A. Dutta, *Overcoming platinum resistance in preclinical models of ovarian cancer using the neddylation inhibitor MLN4924.* Mol Cancer Ther, 2013. **12**(10): p. 1958-67.
34. V. Vichai and K. Kirtikara, *Sulforhodamine B colorimetric assay for cytotoxicity screening.* Nature Protocols, 2006. **1**(3): p. 1112-6.
35. T.C. Chou and P. Talalay, *Quantitative analysis of dose-effect relationships: the combined effects of multiple drugs or enzyme inhibitors.* Adv Enzyme Regul, 1984. **22**: p. 27-55.
36. B. Gyorffy, A. Lanczky, and Z. Szallasi, *Implementing an online tool for genome-wide validation of survival-associated biomarkers in ovarian-cancer using microarray data from 1287 patients.* Endocr Relat Cancer, 2012. **19**(2): p. 197-208.
37. J. Tang, R.L. Erikson, and X. Liu, *Checkpoint kinase 1 (Chk1) is required for mitotic progression through negative regulation of polo-like kinase 1 (Plk1).* Proc Natl Acad Sci U S A, 2006. **103**(32): p. 11964-9.
38. Q. Ling, W. Shi, C. Huang, J. Zheng, Q. Cheng, K. Yu, S. Chen, H. Zhang, N. Li, and M. Chen, *Epigenetic silencing of dual oxidase 1 by promoter hypermethylation in human hepatocellular carcinoma.* Am J Cancer Res, 2014. **4**(5): p. 508-17.
39. W. Zhu, Y. Chen, and A. Dutta, *Rereplication by depletion of geminin is seen regardless of p53 status and activates a G2/M checkpoint.* Molecular and Cellular Biology, 2004. **24**(16): p. 7140-50.
40. C.W. Chen, M.H. Wu, Y.F. Chen, T.Y. Yen, Y.W. Lin, S.H. Chao, S. Tala, T.H. Tsai, T.L. Su, and T.C. Lee, *A Potent Derivative of Indolizino[6,7-b]Indole for Treatment of Human Non-Small Cell Lung Cancer Cells.* Neoplasia, 2016. **18**(4): p. 199-212.
41. A.A. Jazaeri, E. Shibata, J. Park, J.L. Bryant, M.R. Conaway, S.C. Modesitt, P.G. Smith, M.A. Milhollen, A.J. Berger, and A. Dutta, *Overcoming platinum resistance in preclinical models of ovarian cancer using the neddylation inhibitor MLN4924.* Molecular Cancer Therapeutics, 2013. **12**(10): p. 1958-67.
42. S.P. Langdon, S.S. Lawrie, F.G. Hay, M.M. Hawkes, A. McDonald, I.P. Hayward, D.J. Schol, J. Hilgers, R.C. Leonard, and J.F. Smyth, *Characterization and properties of nine human ovarian adenocarcinoma cell lines.* Cancer Res, 1988. **48**(21): p. 6166-72.
43. A. Blasina, J. Hallin, E. Chen, M.E. Arango, E. Kraynov, J. Register, S. Grant, S. Ninkovic, P. Chen, T. Nichols, P. O'Connor, and K. Anderes, *Breaching the DNA damage checkpoint via PF-00477736, a novel small-molecule inhibitor of checkpoint kinase 1.* Mol Cancer Ther, 2008. **7**(8): p. 2394-404.
44. S.D. Zabludoff, C. Deng, M.R. Grondine, A.M. Sheehy, S. Ashwell, B.L. Caleb, S. Green, H.R. Haye, C.L. Horn, J.W. Janetka, D. Liu, E. Mouchet, S. Ready, J.L. Rosenthal, C. Queva, G.K. Schwartz, K.J. Taylor, A.N. Tse, G.E. Walker, and A.M. White, *AZD7762, a novel checkpoint kinase inhibitor, drives checkpoint abrogation and potentiates DNA-targeted therapies.* Mol Cancer Ther, 2008. **7**(9): p. 2955-66.
45. M.K. Kim, J. James, and C.M. Annunziata, *Topotecan synergizes with CHEK1 (CHK1) inhibitor to induce apoptosis in ovarian cancer cells.* BMC Cancer, 2015. **15**: p. 196.
46. T. Seto, T. Esaki, F. Hirai, S. Arita, K. Nosaki, A. Makiyama, T. Kometani, C. Fujimoto, M. Hamatake, H. Takeoka, F. Agbo, and X. Shi, *Phase I, dose-escalation study of AZD7762 alone and in combination with gemcitabine in Japanese patients with advanced solid tumours.* Cancer Chemother Pharmacol, 2013. **72**(3): p. 619-27.
47. G.R. Stark and W.R. Taylor, *Analyzing the G2/M checkpoint.* Methods Mol Biol, 2004. **280**: p. 51-82.

48. C.Z. Zhang, A. Spektor, H. Cornils, J.M. Francis, E.K. Jackson, S. Liu, M. Meyerson, and D. Pellman, *Chromothripsis from DNA damage in micronuclei.* Nature, 2015. **522**(7555): p. 179-84.
49. N.P. Singh, M.T. McCoy, R.R. Tice, and E.L. Schneider, *A simple technique for quantitation of low levels of DNA damage in individual cells.* Exp Cell Res, 1988. **175**(1): p. 184-91.
50. G. Samimi, R. Safaei, K. Katano, A.K. Holzer, M. Rochdi, M. Tomioka, M. Goodman, and S.B. Howell, *Increased expression of the copper efflux transporter ATP7A mediates resistance to cisplatin, carboplatin, and oxaliplatin in ovarian cancer cells.* Clin Cancer Res, 2004. **10**(14): p. 4661-9.
51. R. Safaei, S. Otani, B.J. Larson, M.L. Rasmussen, and S.B. Howell, *Transport of cisplatin by the copper efflux transporter ATP7B.* Mol Pharmacol, 2008. **73**(2): p. 461-8.
52. N. Dehne, J. Lautermann, F. Petrat, U. Rauen, and H. de Groot, *Cisplatin ototoxicity: involvement of iron and enhanced formation of superoxide anion radicals.* Toxicol Appl Pharmacol, 2001. **174**(1): p. 27-34.
53. K.H. Kim, J.Y. Park, H.J. Jung, and H.J. Kwon, *Identification and biological activities of a new antiangiogenic small molecule that suppresses mitochondrial reactive oxygen species.* Biochem Biophys Res Commun, 2011. **404**(1): p. 541-5.
54. J.D. Charrier, S.J. Durrant, J.M. Golec, D.P. Kay, R.M. Knegtel, S. MacCormick, M. Mortimore, M.E. O'Donnell, J.L. Pinder, P.M. Reaper, A.P. Rutherford, P.S. Wang, S.C. Young, and J.R. Pollard, *Discovery of potent and selective inhibitors of ataxia telangiectasia mutated and Rad3 related (ATR) protein kinase as potential anticancer agents.* J Med Chem, 2011. **54**(7): p. 2320-30.
55. S. Chen, X. Chen, G. Xie, Y. He, D. Yan, D. Zheng, S. Li, X. Fu, Y. Li, X. Pang, Z. Hu, H. Li, W. Tan, and J. Li, *Cdc6 contributes to cisplatin-resistance by activation of ATR-Chk1 pathway in bladder cancer cells.* Oncotarget, 2016. **7**(26): p. 40362-40376.
56. C.C. Li, J.C. Yang, M.C. Lu, C.L. Lee, C.Y. Peng, W.Y. Hsu, Y.H. Dai, F.R. Chang, D.Y. Zhang, W.J. Wu, and Y.C. Wu, *ATR-Chk1 signaling inhibition as a therapeutic strategy to enhance cisplatin chemosensitivity in urothelial bladder cancer.* Oncotarget, 2016. **7**(2): p. 1947-59.
57. L. Kelland, *The resurgence of platinum-based cancer chemotherapy.* Nat Rev Cancer, 2007. **7**(8): p. 573-84.

Figure legends

Figure 1. ATR-Chk1 is activated in cisplatin resistant or recurrent ovarian tumors from patients.

(A) Schematics illustrating the combination of qHTCS and genomic sequencing to identify pathways regulating cisplatin resistance and compounds to overcome the resistance. (B) Viability of SKOV3 and SKOV3 CR cells (upper panel), PEO14 and PEO23 (lower panel) treated with increasing concentrations of cisplatin for 3 days. (C) The heatmap of second-round drug screening results based on drug-category-response scores of IC_{50}. The values are logarithm (base 10) of IC_{50} for the compounds or combined with 20 μM of Cisplatin. Two Chk1 inhibitors exhibit enhanced cell killing effect in resistant cells when combined with cisplatin (20 μM). (D) Venn diagram indicating the overlap of genes identified from the Chk1 functional gene set and up-regulated genes set in SKOV3 CR compared with SKOV3 cells (upper panel). The heatmap (lower panel) showed 108 overlapped genes (ATR-Chk1 signature gene set). Colors in the heatmap represent the gene expression levels after z-score normalization across different samples. (E) Cellular pathways regulated by ATR-Chk1 signature genes. (F) Kaplan-Meier curves of 5-year overall survival rate (OS, upper panel) and progression-free survival rates (PFS, lower panel) based on clinical and molecular data for ovarian cancer patients. The patients were stratified by the expression levels in their tumors of the ATR-Chk1 signature genes. Medium survival, Log-rank (Mantel-Cox) *p* values and hazard ratios (HR); 95 % confidence interval in parentheses) are shown. (G) Expression levels of pATR by IHC from the same ovarian patients (upper panel). The IHC quantification of pATR in platinum sensitive and recurrent tumor samples from seven patients. Data are represented as mean ± SD. S, platinum-sensitive ovarian cancer patients; R, platinum-resistant/recurrent ovarian cancer patients. Representative IHC images of pATR in platinum sensitive and recurrent tumor samples (lower panel). Scale bar, 100 μm. (H) Representative IHC images of pATR in platinum sensitive and resistant tumor samples from Patient 1.

Figure 2. Chk1 inhibitors synergistically suppresses cisplatin resistant ovarian cancer cells growth.

(A) The synergistic effects of PF-47336 and cisplatin in SKOV3 CR cells. Concentrations and CI values were presented below the bars. (B) The synergistic effects of AZD7762 and cisplatin in SKOV3 CR cells. Concentrations and CI values were presented below the bars. (C) The synergistic effects of PF-47336 and cisplatin in PEO23 cells. Concentrations and CI values were presented below the bars. (D) The synergistic effects of PF-47336 and cisplatin in PEO23 cells. Concentrations and CI values were presented below the bars. (E) Viability of SKOV3 CR cells treated with increasing concentrations of cisplatin for 3 days after Chk1 depletion by siRNA. Data are represented as mean ± SD from three independent experiments performed in triplicate. (F) SKOV3 CR cells treated as indicated were harvested for FACS analysis to examine apoptosis.

Figure 3. Inhibition of ATR overcomes cisplatin resistance in ovarian cancer cells

(A) SKOV3, SKOV3 CR, PEO14, and PEO23 cells were harvested for Western blotting for pATR (Thr-1989), ATR, pChk1 (Ser-317), Chk1, and FANCD2. (B) Colony formation of SKOV3 CR cells 14 days after they have been treated with 0.5 μM cisplatin and/or 0.1 μM VE-821. Colonies were stained with crystal violet. Data are represented as mean ± SD from three independent experiments performed in triplicate. ***, $p < 0.001$; n.s., not significant. (C) The synergistic effects of VE-821 and cisplatin on SKOV3 CR cells. Concentrations and CI values were presented below the bars. (D) The synergistic effects of VE-821 and cisplatin on PEO23 cells. Concentrations and CI values were presented below the bars. (E) SKOV3 CR cells treated as indicated were harvested for Western blotting for pATR (Thr-1989), ATR, pChk1 (Ser-317), and Chk1. (F) Cells treated as indicated were harvested for FACS analysis to examine the apoptosis (upper panel). SKOV3 CR cells treated as indicated were harvested for Western blotting for PARP-1 and Actin (lower panel).

Figure 4. G2/M checkpoint is activated in cisplatin resistant cells

(A) SKOV3 or SKOV3 CR cells were harvested for cell-cycle analysis. The percentages of each cell-cycle stages were indicated. (B) SKOV3 and SKOV3 CR cells were harvested for Western blotting for pCdc2 (Tyr-15), Cdc2, pH3 (Ser-10), and H3. (C) Metaphase chromosome spread of SKOV3 or SKOV3 CR cells treated with control or cisplatin. The percentages of DNA breakage were indicated. (D) Micronuclei of SKOV3 or SKOV3 CR cells treated with control or Aphidcolin. The percentages of micronuclei population were indicated.

Figure 5. Cisplatin resistant ovarian cancer cells exhibited elevated ability to repair DNA damage.

(A) Modified comet assay to examine ICLs in SKOV3 or SKOV3 CR cells. (B) SKOV3 CR cells treated as indicated were harvested for Western blotting for ATP7A and ATP7B. (C) Cells treated with 10 μM cisplatin were released into cisplatin-free medium and then collected for modified comet assay at indicated time points. Representative images from modified comet assay (left panel). Relative percentage of ICLs in cells treated with cisplatin at indicated time points (right panel). (D) Cells treated with 10 μM cisplatin were released to cisplatin-free medium and then harvested at indicated time points for western blotting for FANCD2 (L-FANCD2, mono-ubiquitinated form; S-FANCD2, unmodified form). (E) Quantification of ratio of L/S-FANCD2 in cells treated as in C. (F) Cells treated with 10 μM cisplatin were released to cisplatin-free medium and then harvested at indicated time points for Western blotting for indicated proteins. (G) Quantification of the levels of phosphorylation of Chk1 in cells treated as in F.

Figure 6. DUOXA1 overexpression sustains increased ROS level in cisplatin resistant ovarian cancer cells.

(A) Representative images of reactive oxygen species (ROS) production in SKOV3, SKOV3 CR, PEO14 and PEO23 cells (upper panel, scale bar, 100 μm). Quantification of relative ROS level in tested cells (lower panel). Data are represented as mean ± SD from three independent experiments performed in triplicate. ***, $p < 0.001$. (B) ROS production in SKOV3 CR and PEO23 cells after treated with the ROS inhibitor YCG063 20 μM for 24 hours (upper panel; scale bar, 100 μm). Quantification of relative ROS level in tested cells (lower panel). Data are represented as mean ± SD from three independent experiments performed in triplicate. ***, $p < 0.001$. (C) SKOV3 CR and PEO23 cells treated with YCG063 20 μM for 24 hours were harvested for Western blotting for indicated proteins. (D) SKOV3 CR cells treated with indicated compounds were harvested for Western blotting for indicated proteins. (E) Heatmap of genes that are involved in ROS pathway and up-regulated in resistant cells. Colors in the heat-map represent the gene expression levels after z-score normalization across different samples. (F) qPCR to examine DUOXA1 expression in indicated cells. Data are represented as mean ± SD from three independent experiments performed in triplicate. ***, $p < 0.001$. (G) SKOV3, SKOV3 CR, PEO14 and PEO23 were harvested for Western blotting for DUOXA1. (H) SKOV3 CR cells transfected with control siGL2 or siDUOXA1 were examined for ROS production (upper panel; scale bar, 100 μm). Quantification of relative ROS level in tested cells (lower panel). Data are represented as mean ± SD from three independent experiments performed in triplicate. ***, $p < 0.001$. (I) SKOV3 CR cells treated as indicated were harvested for pATR (Thr-1989), ATR, pChk1 (Ser-317), and Chk1. (J) Viability of SKOV3 CR cells treated with increasing concentrations of cisplatin for 3 days after DUOXA1 knockdown. *, $p < 0.05$. (K) SKOV3 CR cells treated as indicated were harvested for FACS analysis to examine apoptosis. (L) Kaplan-Meier curves of 5-year overall survival rate (OS) based on clinical and molecular data for ovarian cancer patients. The patients were stratified by the expression levels of DUOXA1 in their tumors. Medium survival, Log-rank (Mantel-Cox) *p* values and hazard ratios (HR); 95 % confidence interval in parentheses) are shown. (M) Expression levels of DUOXA1 by IHC from the same ovarian patients. The IHC quantification of DUOXA1 levels in platinum sensitive and platinum resistance tumor samples from seven patients. Data are represented as mean ± SD.

Figure 7. ATR inhibition suppresses SKOV3 CR xenograft tumor growth

(A) Growth curves of SKOV3 CR xenograft tumors treated with vehicle, VE-822 (oral gavage at 60 mg/kg on days 1, 2, 3, 5, 6, 7, 9, 10, and 11), cisplatin (6 mg/kg intraperitoneally on days 1, 5, and 9), or VE-822 plus cisplatin (Combo) for 2 weeks. Data are represented as means ± SEM, n = 6 mice/group. **, $p < 0.01$, ***, $p < 0.001$ by two-way ANOVA. The right panel is the photograph of the representative tumors from mice at treatment on day 24. Ruler scale is in cm. (B) Representative hematoxylin and eosin (H&E) staining of samples of xenograft tumors, livers, and kidneys from mice treated with cisplatin and/or VE-822. Specimens were collected on day 20. (C) IHC staining of pATR in samples of xenograft tumors collected on 4 days after the last treatment. *, $p < 0.05$; **, $p < 0.01$; n.s., not significant. (D) *In situ* apoptosis analysis of xenograft tumors collected on 4 days after the last treatment using TUNEL assay. *, $p < 0.05$; **, $p < 0.01$; ***, $p < 0.001$. Scale bar, 100um for H&E and pATR IHC, 50 μm for TUNEL. (E) Working model of DUOXA1-medaited ROS production in the regulation of cisplatin resistance in ovarian cancer.

Supplementary information

DUOXA1-mediated ROS production promotes cisplatin resistance by activating ATR-Chk1 pathway in ovarian cancer

Yunxiao Meng, Chi-Wei Chen, Mingo MH Yung, Wei Sun, Jing Sun, Zhuqing Li, Jing Li, Zongzhu Li, Wei Zhou, Stephanie S Liu, Annie NY Cheung, Hextan YS Ngan, John C. Braisted, Yan Kai, Weiqun Peng, Alexandros Tzatsos, Yiliang Li, Zhijun Dai, Wei Zheng, David W. Chan, Wenge Zhu

Appendix S1

Cell lines and generation of resistant cells The cisplatin sensitive SKOV3 cells was treated with cisplatin for six cycles (4 hours of cisplatin treatment, followed by release to cisplatin free medium for three weeks). Only early-passage (<10 passages) SKOV3 CR cells were used for the study. All cells were cultured at 37 °C in a humidified incubator containing 5% CO_2.

Antibodies and reagents anti-ATR (SC-1887), anti-FANCD2 (SC-20022), anti-ATP7A (SC-376467), and anti-ATP7B (SC-373964) were from Santa Cruz Biotechnology, anti-pChk1 (Ser-317, # 2344), anti-Chk1 (#2360), anti-PARP-1 (#9542), anti-γH2AX (#9718) and anti-H2AX (#7631) were from Cell Signaling Technology, anti-pATR (GTX128145, phospho Thr-1989) was from GeneTex, anti-GAPDH (G8795) and anti-Actin (A2228) were from Sigma-Aldrich, and anti-DUOXA1 (26632-1-AP) was from Proteintech. Cisplatin (cis-Diamineplatinum(II) dichloride) and Colcemid and Aphidicolin were from Sigma-Aldrich. VE-821 and VE-822 were from Selleckchem.

YCG063 and MnTmpyp were from Calbiochem. For *in vitro* and *in vivo* experiments, cisplatin was dissolved in sterile saline. VE-821, VE-822 and YCG063 were dissolved in DMSO for *in vitro* experiments. For *in vivo* study, VE-822 was dissolved in solution in 10% Vitamin E Tocopheryl Polyethylene Glycol Succinate (VitE TPGS).

Cell viability assay Cells were plated in 96-well plate at a density of 3000 cells per well and treated with indicated reagents for different concentrations. Three days after treatment, the cell viability was measured by Sulforhodamine B (SRB) assay [1]. The IC_{50} and combinational index (IC) were further determined by compusyn software [2]. Experiments were conducted in triplicate and repeated three times.

Quantitative high throughput combinational screen (qHTCS) An ATP content cell viability assay kit was purchased from Promega. Polystyrene plates (1536-well white, solid bottom, sterile, tissue culture treated) were purchased from Greiner Bio-One. Compounds and cisplatin were freshly prepared in 0.9% sodium chloride. Cell viability was measured using a luciferase-based ATP content assay as described previously [3]. Briefly, cisplatin resistant ovarian cancer cells SKOV3 CR were plated at 1500 cells/well in 5 µL assay medium (DMEM + 10% FBS) and incubated for 16 hours at 37 °C with 5% CO_2. Compounds and/or cisplatin was premixed in assay medium, and 1 µL of this mixture was then transferred into assay plate using Multidrop Combi (Thermo Fisher Scientific); 23 nL of the second drug in 1536-well compound plate was transferred into the assay plate using NX-TR pin tool station (WAKO Scientific Solutions). After incubation at 37 °C with 5% CO_2 for 72 hours, 4 µL/well ATP detection solution was added into the assay plate using Multidrop Combi. 30 min after incubation at room temperature, the luminescence signal was measured using

ViewLux plate reader (PerkinElmer).The primary screen data and curve fitting were analyzed using software developed internally at the NIH Chemical Genomics Center (NCGC) [4]. Heatmap of drug combinations where columns enumerate cisplatin/vehicle, rows enumerate the other drug, and heat map elements are half maximal inhibitory concentration (IC_{50}). The IC_{50} values were computed by fitting the concentration response titrations (using the normalized, corrected signal) to the Hill equation from which the IC_{50} value was calculated as the concentration at which the fitted curve reaches 50% of maximum. IC_{50} values were calculated using Prism software (GraphPad).

RNA-sequencing (RNA-seq) Fragmented RNA was converted into double-stranded cDNA, which was further employed as a template for PCR using four fluorescently labeled nucleotides. Fluorescence was measured for each cluster during each cycle to identify the base that was added to each cluster. Read counts of each sample were normalized with DESeq and ran against their negative binomial two sample test to find significant genes that higher transcript abundance in either the SKOV3 or SKOV3 CR. Genes with false discovery rate (FDR) < 0.05, fold change larger than 2 or smaller than 0.5-fold were considered as differentially expressed genes.

Kaplan-Meier plotter Using the platform (http://kmplot.com, [5]) to analyze GSE and TCGA databases, we input the 108 signature genes. We set auto select best cutoff and restricted analysis to treatment groups receiving chemotherapy containing platin (1259 patients). The array quality control is excluded biased arrays.

Specimens of ovarian cancer patients The specimens of chemosensitive and

matched recurrent or chemoresistant tumor tissues from ovarian cancer patients were kept as formalin-fixed paraffin-embedded (FFPE) samples in the Department of Pathology at University of Hong Kong. Studies using human tissues were approved by the local institutional ethics committee (institutional review board reference No: UW 05-143 T/806 and UW 11-298). Written informed consent was received from patients prior to their inclusion in the study. The histological types, disease stages, and cancer cell contents in each FFPE sections were examined by the experienced pathologists.

Immunohistochemistry Paraffin tissue sections were deparaffinized in xylene and rehydrated with gradient alcohol solutions. Antigen-retrieval treatment was performed using 10 mM sodium citrate buffer (pH 6.0) at 121 °C for 5 minutes. Slides were then treated with 3% hydrogen peroxide in methanol solution for 10-15 minutes to quench endogenous peroxidase activity. 10% normal goat serum was used to block nonspecific bindings for 30 minutes. For the primary antibody, the slides were incubated at 4 °C overnight. SuperPicture™ Polymer Detection Kit (Thermo Fisher Scientific) cells was for the second antibody incubation and 3'-Diaminobenzidine (DAB) staining according to the manufacturer's instructions. Finally, the slides were lightly counterstained with hematoxylin. For quantification, immunoreactivity was evaluated semiquantitatively by the staining intensity and proportion. The proportion of staining was scored from 0 to 3 as follows: 3, >50% of cells positive; 2, 10%–49%; 1, <10%. Staining intensity was scored from 0 to 3 (0, absent; 1, weak; 2, moderate; 3, intense). The final IHC score for each sample was determined by multiplying the intensity and the proportion of stained cells. The analysis was undertaken blindly by 2 independent people.

siRNA interference siChk1 (5'-AAGCGTGCCGTAGACTGTCCA-3'), DUOXA1 (5'-GGACUUAUCCUGGCUAGAG-3'), and a negative control (siGL2) were as described previously [6-8]. Cells were transfected with siRNA using Lipofectamine RNAiMAX (Thermo Fisher Scientific) according to the manufacturer's instructions. Cells were harvested for analyses 48 hours after siRNA transfection.

Flow cytometry FITC Annexin-V Apoptosis Detection Kit (BD Pharmingen) was used for the apoptosis analysis according to the manufacturer's instructions. Briefly, cells were treated with the indicated agents for 48 hours and then digested with 0.25% trypsin, followed by washing with cold PBS twice and then re-suspended in 1X binding buffer at 1 x 10^6 cells /ml. 5 µl of Annexin-V FITC and 5 µl of propidium iodide (PI) were added to 100 µl of the cell suspension (1 x 10^5 cells). The apoptotic cells populations were then analyzed by flow cytometry (Celestra, BD Biosciences). Cell cycle analysis was performed as previous description [9]. The distributions of cell cycle phases were determined using Flowjo software.

Clonogenic cell survival assay Cells were plated in 6-well dishes at a density of 250-300 cells per dish, and then were treated with the drugs at indicated concentrations. Cells were then kept in the incubator for 14 days to allow colony formation. After medium removal, cells were stained with 0.5% crystal violet. Colonies with more than 50 cells were counted.

Metaphase chromosome spread Cells were incubated with 1 µg/ml Colcemid at 37 °C for one hour. After washed with PBS, cells were then treated with ice cold 0.56% KCl at room temperature for 6 minutes, followed by the fixation with methanol:

glacial acetic acid (3:1) and then seeded onto glass slides. DNA was visualized on microscope after staining with DAPI for observation of chromosome integrity using a microscope. Immunofluorescence for micronuclei study was performed on cells grown on coverslips in 6-well plates. Cells containing micronuclei were analyzed after staining with DAPI.

Modified comet assay The experiment was performed according to the manufacture's instruction of CometAssay® Kit (Trevigen). Cells were treated with/without cisplatin at 10 μM before released to fresh medium. The cells were then treated with γ-radiation (20 Gy) to break DNA into fragments. Cells (1000/10 μL in PBS) were mixed with 100 μL low-melting point agarose and were applied on CometAssay Kit slides. After cells were lysed in lysis buffer, slides were electrophoresed at 300 mA and 20 voltages for 55 minutes. The tail moments were stained with SYBR Geen® I and at least 50 cells were analyzed with OpenComet software. The following formula was used for the calculation of ICLs. Percentage of DNA with ICLs = [1 – (TMdi − TMcu/TMci −TMcu)] × 100%. TMdi is tail moment of drug-treated irradiated sample, TMcu is tail moment of untreated non-irradiated control, and TMci is tail moment of untreated irradiated control.

Reactive Oxygen Species (ROS) detection A live cell-permeable, fluorophore CellROX Orange reagent (Thermo Fisher Scientific) was used to detect the cellular ROS level according to the manufacturer's instructions.

qPCR Isolation of RNA and reverse transcription of cDNA were conducted by following the instructions of Qiagen miRNeasy Mini Kita and Bio-Rad iScript cDNA

Synthesis Kits. The qPCR was performed with Real-Time PCR Supermixes and Kits. Primers were syntheszied from Sigma for detecting DUOXA1 (forward: 5'-CATTCCTCTGCTGGCTACTG-3'; reverse: 5'-AGCATGTGGCCACCATAAAC-3 [10]) by qPCR.

Animal experiments Animal housing and all procedures were conducted with protocols approved by the Institutional Animal Care and Use Committees (IACUC) of The George Washington University. In brief, 5-6 weeks old female BALB/c athymic nude mice (The Jackson Laboratory; weighting 20-25 g) were inoculated subcutaneously by injecting the cisplatin resistant cell line (SKOV3 CR) suspended in 100 µl ice-cold Matrigel/PBS (1:1, V:V; 5 x 10^6/mouse) into the dorsal flank of each mouse. The mice were randomized group into subsequent experiment groups of 8 mice when tumor volume reached 100-150 mm^3 in average. Cisplatin was then given intraperitoneally at 6 mg/kg on day 1, 5, and 9. VE-822 was administrated via oral gavage at 60 mg/kg in 10% VitE TPGS on day 1, 2, 3, 5, 6, 7, 9, 10, and 11. Tumors were measured twice a week. The relative tumor volumes were calculated according to the formula: Length ×($Width^2$) / 2, (length is the longest diameters and width is shortest diameters). Animals were sacrificed when tumors reached 1.5 cm^3 or when they showed any signs of distress (e.g., breathing disorders, weight loss, or immobility) according to institutional criteria. In the case of combination therapy experiments, mice were randomly assigned to the same treatment groups and treated by the same protocol. Tumors were collected 4 days after final administration for subsequent experiment and evaluation.

TUNEL assay TUNEL assay were conducted by following the instruction of In Situ Cell

Death Detection Kit (Roche) to detect apoptotic tumor cells *in vivo*. In brief, paraffin tissue sections were deparaffinized in xylene and rehydrated in gradient alcohol solutions. Slides were then incubated with 0.1% Triton X-100 (Sigma-Aldrich) for 8 minutes and then incubated in 3% hydrogen peroxide in PBS (pH 7.4) for 5 minutes. The slides were incubated in terminal deoxyribonucleotide transferase (TdT) at 37 °C for 60 minutes and followed by incubation of horseradish peroxidase (POD) at 37 °C for 30 minutes. DAB Substrate (Thermo Fisher Scientific) was used to demonstrate Peroxidase activity. Slides were counterstained with hematoxylin before observation. At least 2000 cells were counted in random fields with 400-fold magnification under a microscope to quantify apoptosis.

Statistical analysis Each value reported represents the mean ± SEM or mean ± SD as indicated in the Figure legends. For Kaplan Meier survival analysis, a Log-rank (Mantel-Cox) test was used to compare each of the arms. A Student's t-test was used to analysis differences in tumor volumes between two groups. For comparisons between multiple groups, a one-way ANOVA or two-way analysis was used with a Bonferroni post-test. All statistical tests were two-sided. Differences were considered statistically significant at a p value of less than 0.05. All statistical analysis was performed with GraphPad Prism 7.00.

Appendix S2

Supplementary Table S1. Clinical characteristics of primary and recurrent ovarian cancer patient of HKU cohort 3

Patient	Age (Years)	Stage	Histology	Grade	Chemotherapy	PFD after chemo (months)
1	58	IC	Clear cell	3	Carboplatin + Taxol	41
2	50	IIC	Endometrioid	3	Carboplatin + Taxol	34
3	68	IIIC	Serous	N/A	Carboplatin + Taxol	25
4	56	IC	Clear cell	1	Carboplatin + Taxol + Bevacizumab	30
5	54	IIIC	Mucinous	2	Carboplatin + Taxol	11
6	78	IC	Serous	3	Carboplatin	22
7	55	IIIC	Clear cell	3	Carboplatin + Taxol	47

N/A, Not applicable.

Supplementary Table S2. List of ATR-Chk1 signature genes

RPA3	CKS2	PROCR	ASPM	CDC25A	KIF14	ITGB3BP	BRIX1	TMSB15A	SLC35B1	DUT	KIF23
EMG1	CBX5	BIRC5	SIGMAR1	NUP37	ARPP19	PRIM1	DUS4L	LSM5	ZNF268	MCM4	NCAPG2
TMEM5	UNG	RRM2	CCNA2	RAD51AP1	XPO1	UBE2C	GNA13	CCNE2	ZWILCH	FANCI	TLK2
BUB1	SKP2	GJC1	BRCA2	PLK4	PHTF1	PIGK	CCT2	CD3EAP	SMC2	NEK2	CDC6
CBX3	RFC5	DCK	CDCA3	NUPL2	HELLS	NOLC1	NUP107	GGH	HMGN4	RPP30	CCNB2
SNRPF	NCAPH	SNRPD1	ORC6	PBK	CDC7	EXO1	KNTC1	MAD2L1	C1orf112	KIF15	CCT6A
CLP1	FOXM1	ZWINT	ZNF273	CDK6	TXNDC9	NEIL3	TOM1L1	TMPO	KIAA0101	TIPIN	PRIM2
LANCL1	TFAM	DNM1L	STIL	KRR1	HMGXB4	NME6	SLC9A6	BRCA1	DTL	ARHGAP11A	POLQ
TMED2	ZBTB6	NCAPD2	TOPBP1	RNF138	KIF11	DDX18	KIF20B	IGF2BP3	ABCE1	CBX1	MCM10

References

1. V. Vichai and K. Kirtikara, *Sulforhodamine B colorimetric assay for cytotoxicity screening.* Nature Protocols, 2006. **1**(3): p. 1112-6.
2. T.C. Chou and P. Talalay, *Quantitative analysis of dose-effect relationships: the combined effects of multiple drugs or enzyme inhibitors.* Adv Enzyme Regul, 1984. **22**: p. 27-55.
3. J. Kouznetsova, W. Sun, C. Martinez-Romero, G. Tawa, P. Shinn, C.Z. Chen, A. Schimmer, P. Sanderson, J.C. McKew, W. Zheng, and A. Garcia-Sastre, *Identification of 53 compounds that block Ebola virus-like particle entry via a repurposing screen of approved drugs.* Emerg Microbes Infect, 2014. **3**.
4. Y. Wang, A. Jadhav, N. Southal, R. Huang, and D.T. Nguyen, *A grid algorithm for high throughput fitting of dose-response curve data.* Curr Chem Genomics, 2010. **4**: p. 57-66.
5. B. Gyorffy, A. Lanczky, and Z. Szallasi, *Implementing an online tool for genome-wide validation of survival-associated biomarkers in ovarian-cancer using microarray data from 1287 patients.* Endocr Relat Cancer, 2012. **19**(2): p. 197-208.
6. J. Tang, R.L. Erikson, and X. Liu, *Checkpoint kinase 1 (Chk1) is required for mitotic progression through negative regulation of polo-like kinase 1 (Plk1).* Proc Natl Acad Sci U S A, 2006. **103**(32): p. 11964-9.
7. Q. Ling, W. Shi, C. Huang, J. Zheng, Q. Cheng, K. Yu, S. Chen, H. Zhang, N. Li, and M. Chen, *Epigenetic silencing of dual oxidase 1 by promoter hypermethylation in human hepatocellular carcinoma.* Am J Cancer Res, 2014. **4**(5): p. 508-17.
8. W. Zhu, Y. Chen, and A. Dutta, *Rereplication by depletion of geminin is seen regardless of p53 status and activates a G2/M checkpoint.* Molecular and Cellular Biology, 2004. **24**(16): p. 7140-50.
9. S.C. Kolwicz, Jr., G.L. Odom, S.G. Nowakowski, F. Moussavi-Harami, X. Chen, H. Reinecke, S.D. Hauschka, C.E. Murry, G.G. Mahairas, and M. Regnier, *AAV6-mediated Cardiac-specific Overexpression of Ribonucleotide Reductase Enhances Myocardial Contractility.* Mol Ther, 2016. **24**(2): p. 240-250.
10. A. Yoshihara, T. Hara, A. Kawashima, T. Akama, K. Tanigawa, H. Wu, M. Sue, Y. Ishido, N. Hiroi, N. Ishii, G. Yoshino, and K. Suzuki, *Regulation of dual oxidase expression and H2O2 production by thyroglobulin.* Thyroid, 2012. **22**(10): p. 1054-62.

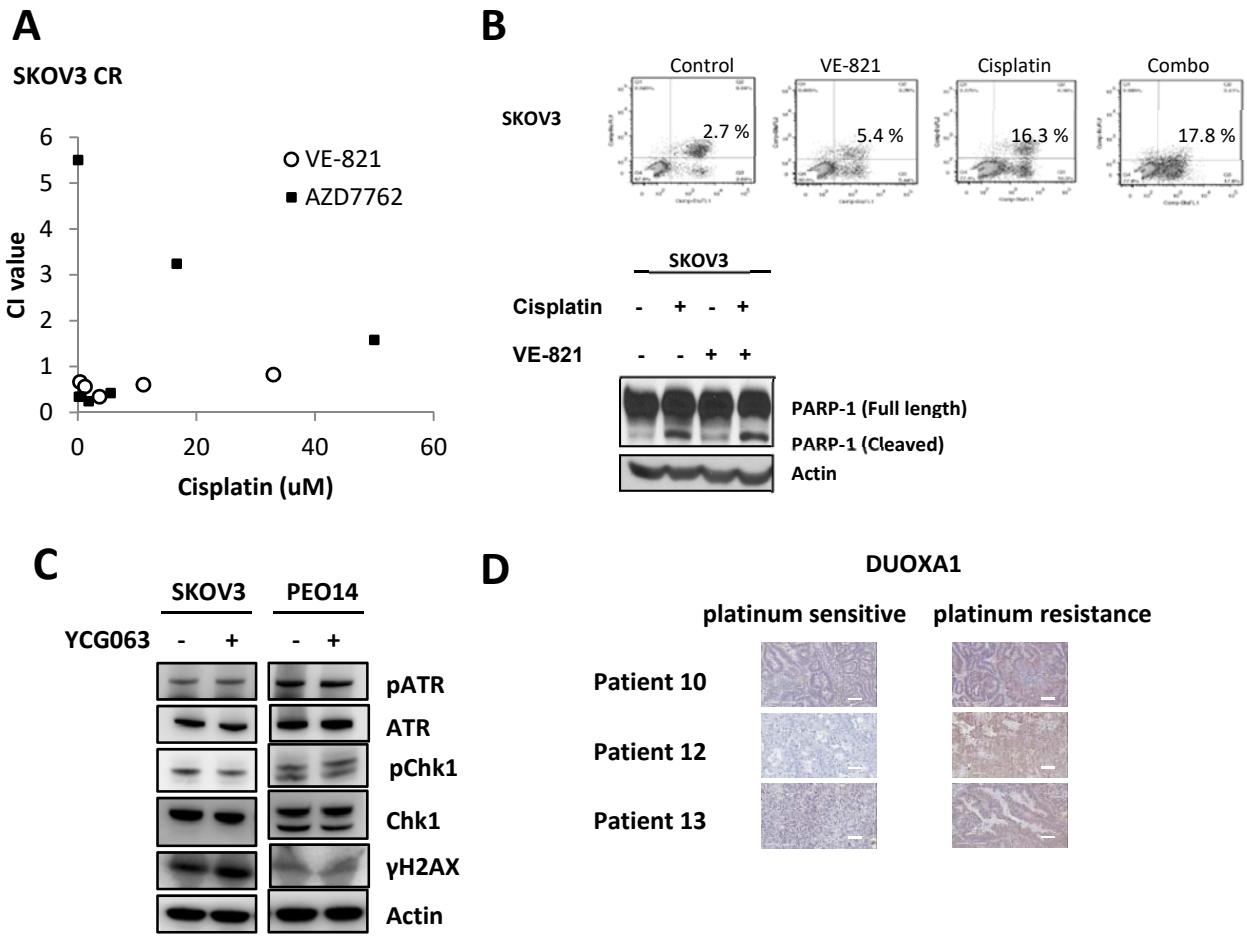

Supplemental Figure 1 (A) CI values of Cisplatin/VE-821 and Cisplatin/AZD7762 against SKOV3 CR. (B) Cells treated as indicated were harvested for FACS analysis (upper panel) and western blotting (lower panel) to examine the apoptosis. (C) Cells treated as indicated were harvested for western blotting for indicated proteins. (D) Representative IHC images of DUOXA1 in platinum sensitive and platinum resistance tumor samples. Scale bar, 100 μm.

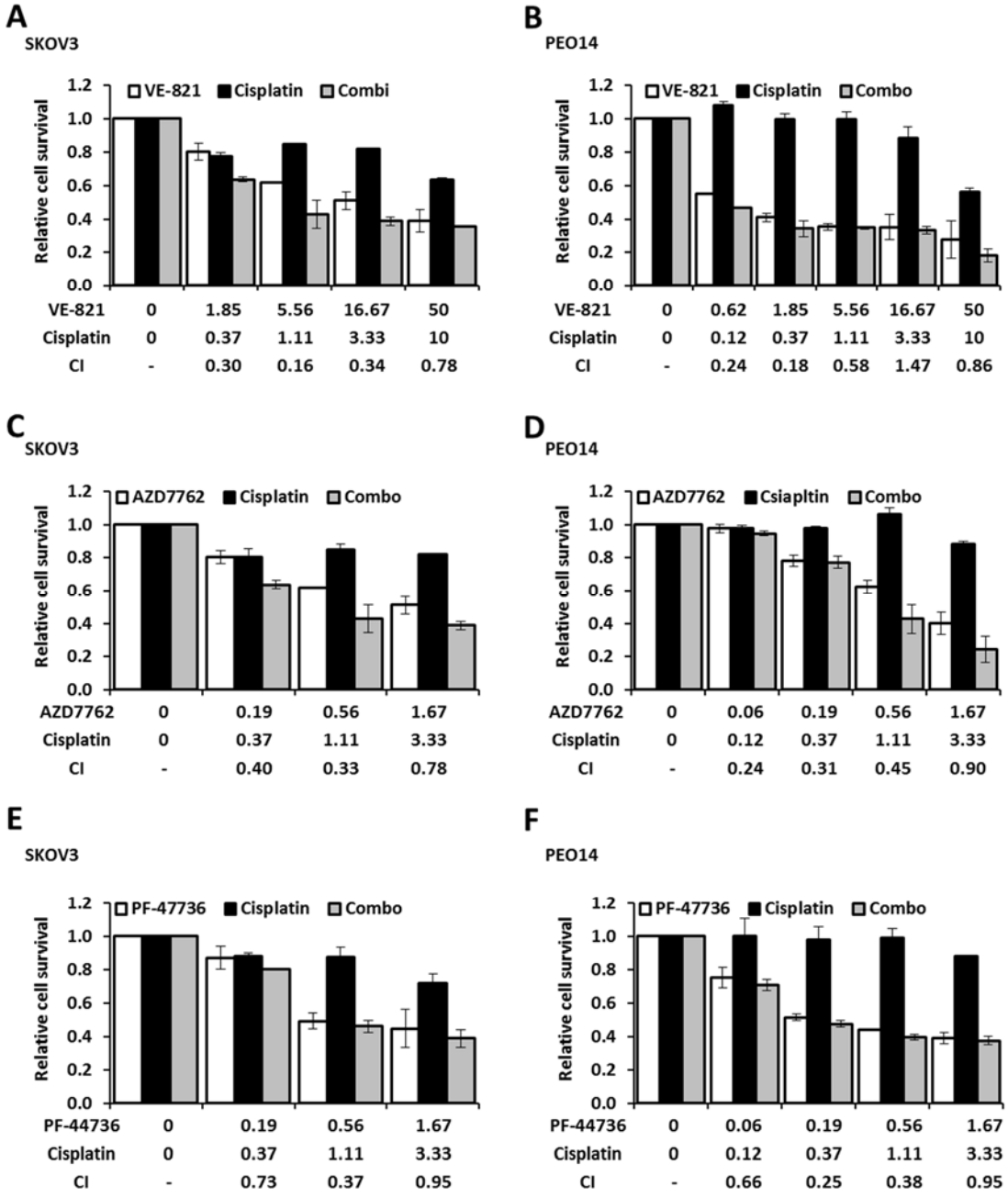

Supplemental Figure 2 (A) The synergistic effects of VE-821 and cisplatin on SKOV3 cells. (B) The synergistic effects of VE-821 and cisplatin on PEO14 cells. (C) The synergistic effects of AZD7762 and cisplatin on SKOV3 cells. (D) The synergistic effects of AZD7762 and cisplatin on PEO14 cells. (E) The synergistic effects of PF-47736 and cisplatin on SKOV3 cells. (F) The synergistic effects of PF-47736 and cisplatin on PEO14 cells. Concentrations and CI values were presented below the bars.

Figure 1

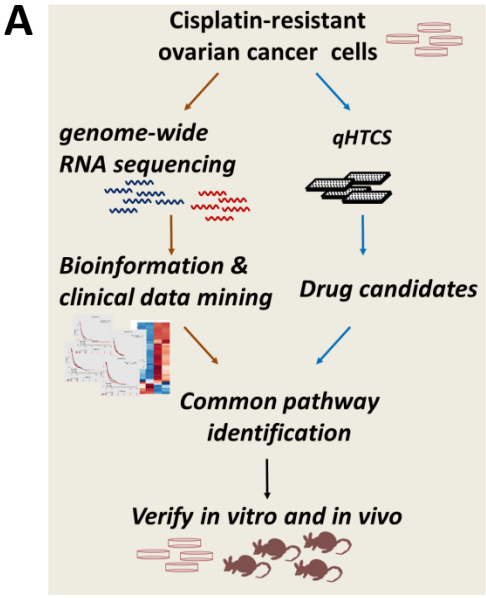

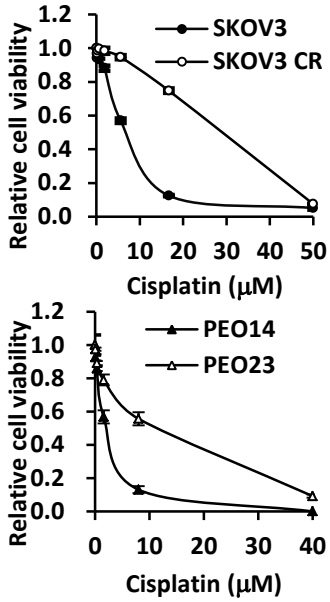

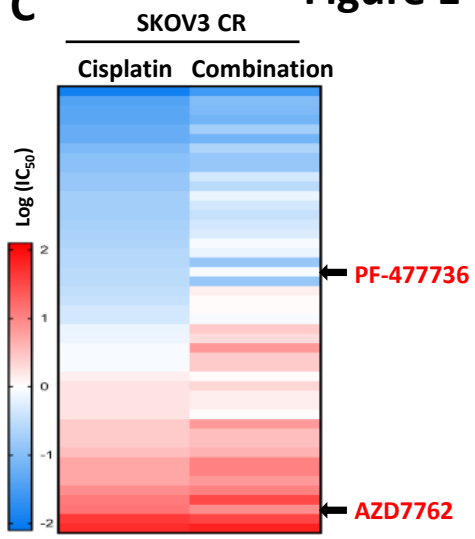

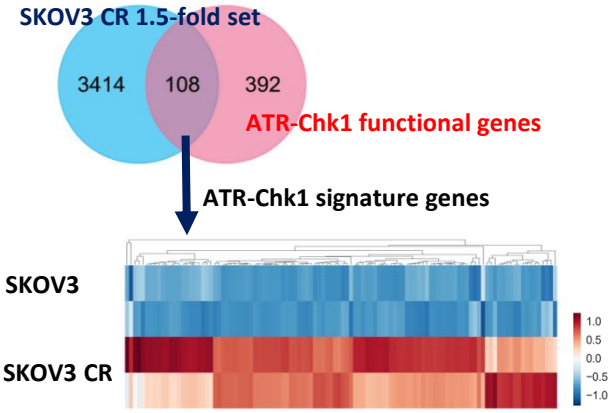

E

KEGG Pathway ID	Pathway description	False discovery rate
04110	Cell cycle	4.16e-10
03030	DNA replication	0.00452
00240	Pymidine metabolism	0.00993
03460	Fanconi anemia pathway	0.00993
03430	Mismatch repair	0.0106
04115	P53 signaling pathway	0.0157

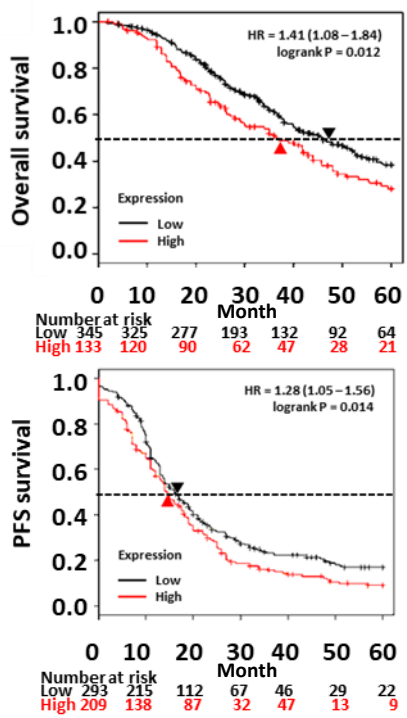

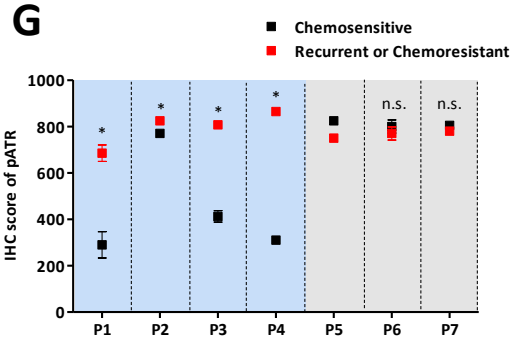

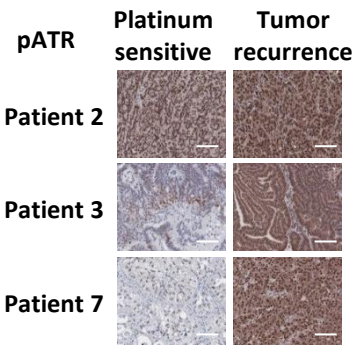

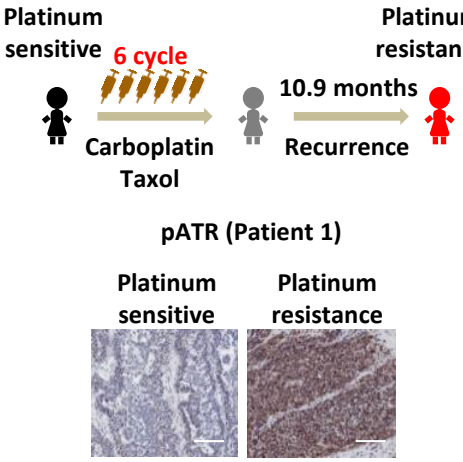

Figure 2

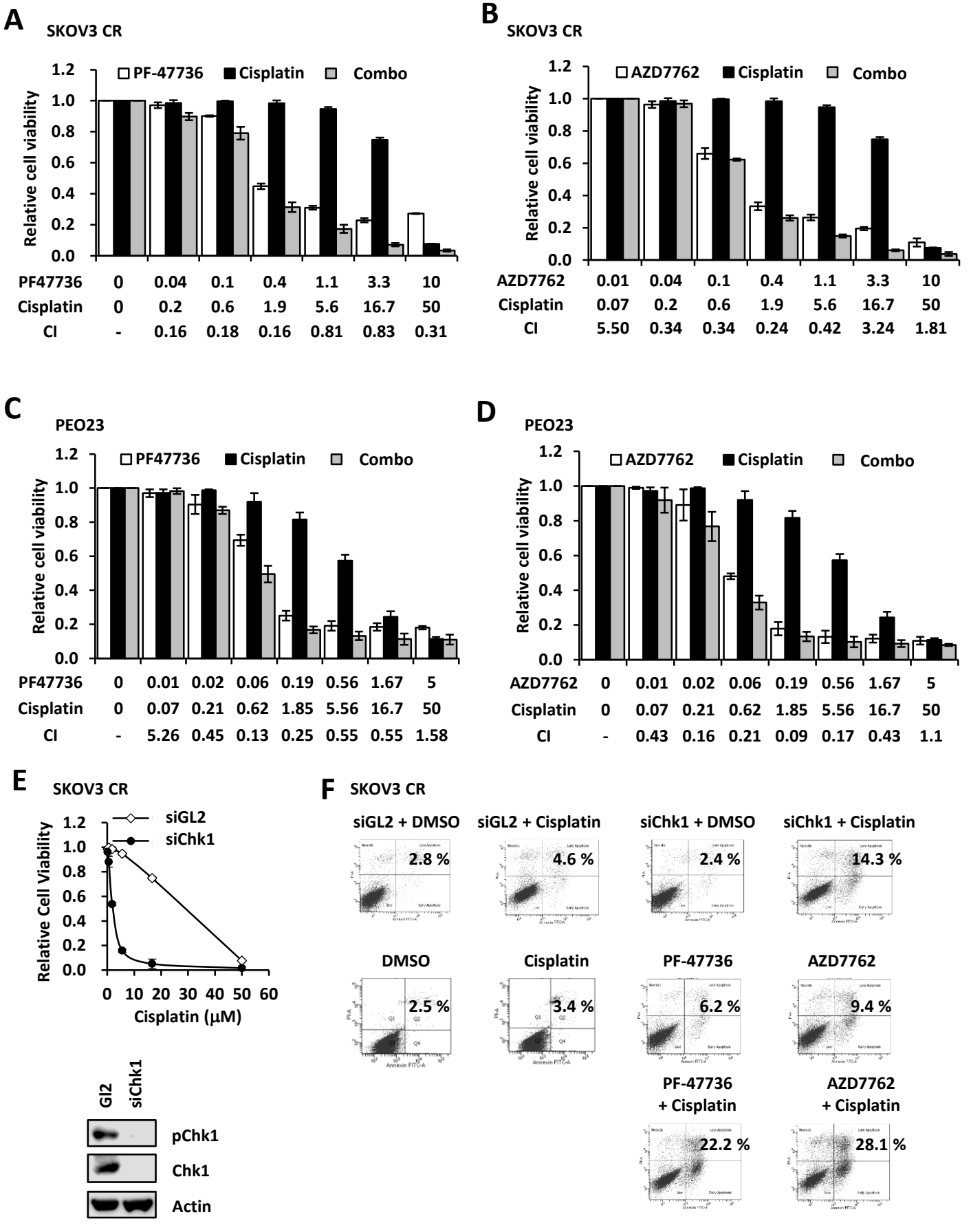
A
SKOV3 CR
PF-47736
Cisplatin
Combo
Relative cell viability
PF47736 0 0.04 0.1 0.4 1.1 3.3 10
Cisplatin 0 0.2 0.6 1.9 5.6 16.7 50
CI - 0.16 0.18 0.16 0.81 0.83 0.31
B
SKOV3 CR
AZD7762
Cisplatin
Combo
Relative cell viability
AZD7762 0.01 0.04 0.1 0.4 1.1 3.3 10
Cisplatin 0.07 0.2 0.6 1.9 5.6 16.7 50
CI 5.50 0.34 0.34 0.24 0.42 3.24 1.81
C
PEO23
PF47736
Cisplatin
Combo
Relative cell viability
PF47736 0 0.01 0.02 0.06 0.19 0.56 1.67 5
Cisplatin 0 0.07 0.21 0.62 1.85 5.56 16.7 50
CI - 5.26 0.45 0.13 0.25 0.55 0.55 1.58
D
PEO23
AZD7762
Cisplatin
Combo
Relative cell viability
AZD7762 0 0.01 0.02 0.06 0.19 0.56 1.67 5
Cisplatin 0 0.07 0.21 0.62 1.85 5.56 16.7 50
CI - 0.43 0.16 0.21 0.09 0.17 0.43 1.1
E
SKOV3 CR
siGL2
siChk1
Relative Cell Viability
Cisplatin (μM)
Gl2
siChk1
pChk1
Chk1
Actin
F
SKOV3 CR
siGL2 + DMSO
2.8 %
siGL2 + Cisplatin
4.6 %
siChk1 + DMSO
2.4 %
siChk1 + Cisplatin
14.3 %
DMSO
2.5 %
Cisplatin
3.4 %
PF-47736
6.2 %
AZD7762
9.4 %
PF-47736 + Cisplatin
22.2 %
AZD7762 + Cisplatin
28.1 %

Figure 3

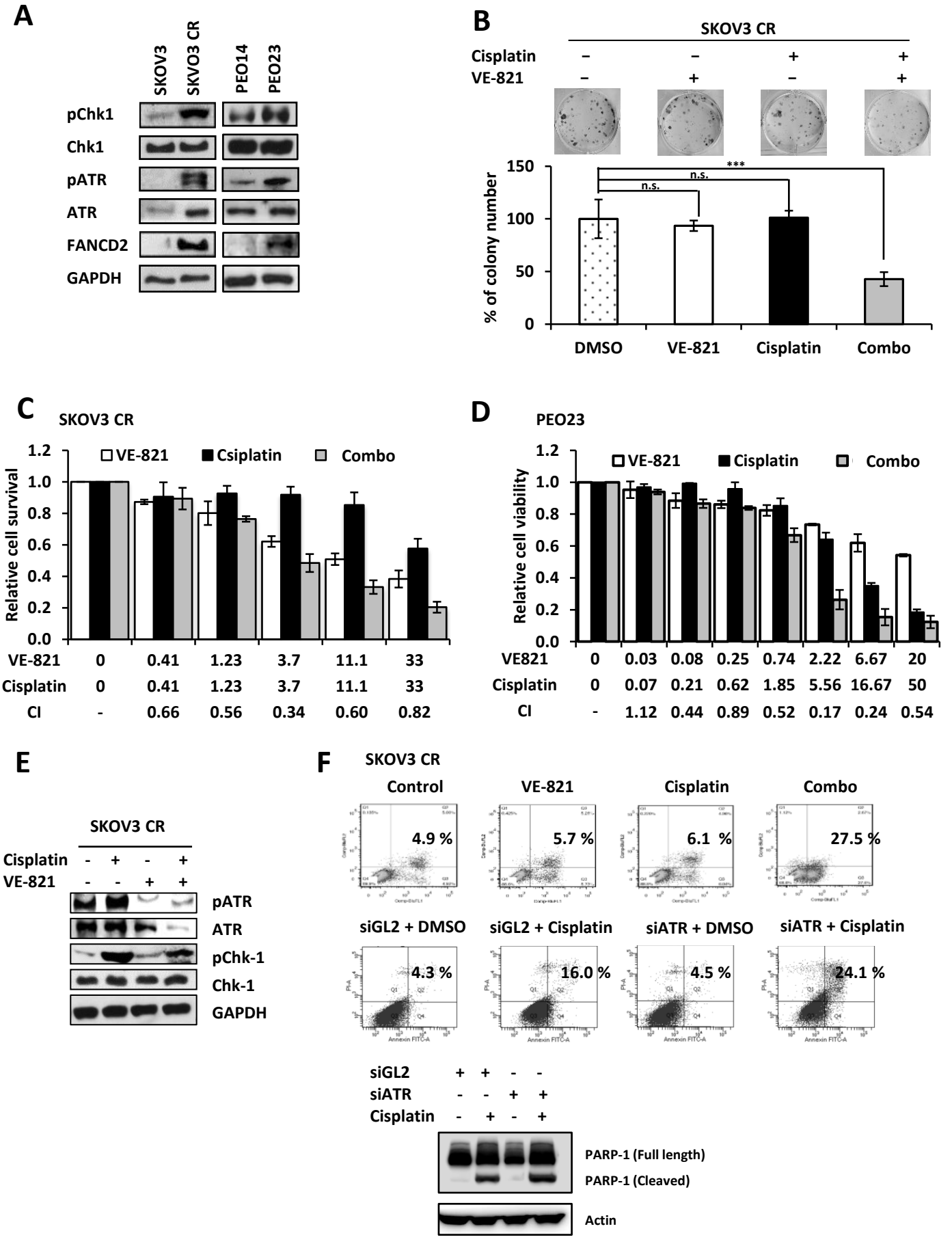
A
SKOV3
SKVO3 CR
PEO14
PEO23
pChk1
Chk1
pATR
ATR
FANCD2
GAPDH
B
SKOV3 CR
Cisplatin – – + +
VE-821 – + – +
% of colony number
150
100
50
0
***
n.s.
n.s.
DMSO
VE-821
Cisplatin
Combo
C
SKOV3 CR
VE-821
Csiplatin
Combo
Relative cell survival
1.2
1.0
0.8
0.6
0.4
0.2
0.0
VE-821 0 0.41 1.23 3.7 11.1 33
Cisplatin 0 0.41 1.23 3.7 11.1 33
CI - 0.66 0.56 0.34 0.60 0.82
D
PEO23
VE-821
Cisplatin
Combo
Relative cell viability
1.2
1.0
0.8
0.6
0.4
0.2
0.0
VE821 0 0.03 0.08 0.25 0.74 2.22 6.67 20
Cisplatin 0 0.07 0.21 0.62 1.85 5.56 16.67 50
CI - 1.12 0.44 0.89 0.52 0.17 0.24 0.54
E
SKOV3 CR
Cisplatin - + - +
VE-821 - - + +
pATR
ATR
pChk-1
Chk-1
GAPDH
F
SKOV3 CR
Control
VE-821
Cisplatin
Combo
4.9 %
5.7 %
6.1 %
27.5 %
siGL2 + DMSO
siGL2 + Cisplatin
siATR + DMSO
siATR + Cisplatin
4.3 %
16.0 %
4.5 %
24.1 %
Annexin FITC-A
siGL2 + + - -
siATR - - + +
Cisplatin - + - +
PARP-1 (Full length)
PARP-1 (Cleaved)
Actin

Figure 4

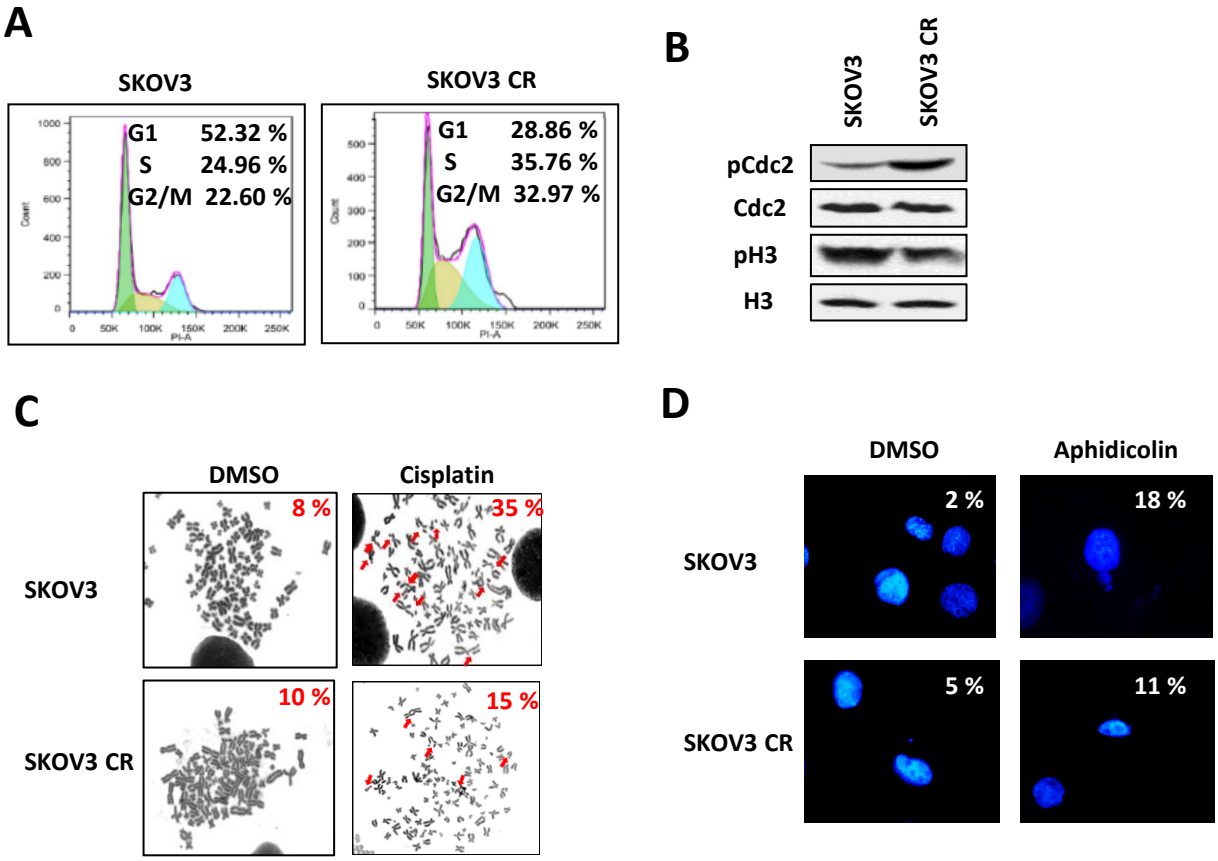
A
SKOV3
SKOV3 CR
G1 52.32 %
S 24.96 %
G2/M 22.60 %
G1 28.86 %
S 35.76 %
G2/M 32.97 %
B
SKOV3
SKOV3 CR
pCdc2
Cdc2
pH3
H3
C
DMSO
Cisplatin
SKOV3
SKOV3 CR
8 %
35 %
10 %
15 %
D
DMSO
Aphidicolin
SKOV3
SKOV3 CR
2 %
18 %
5 %
11 %

Figure 5

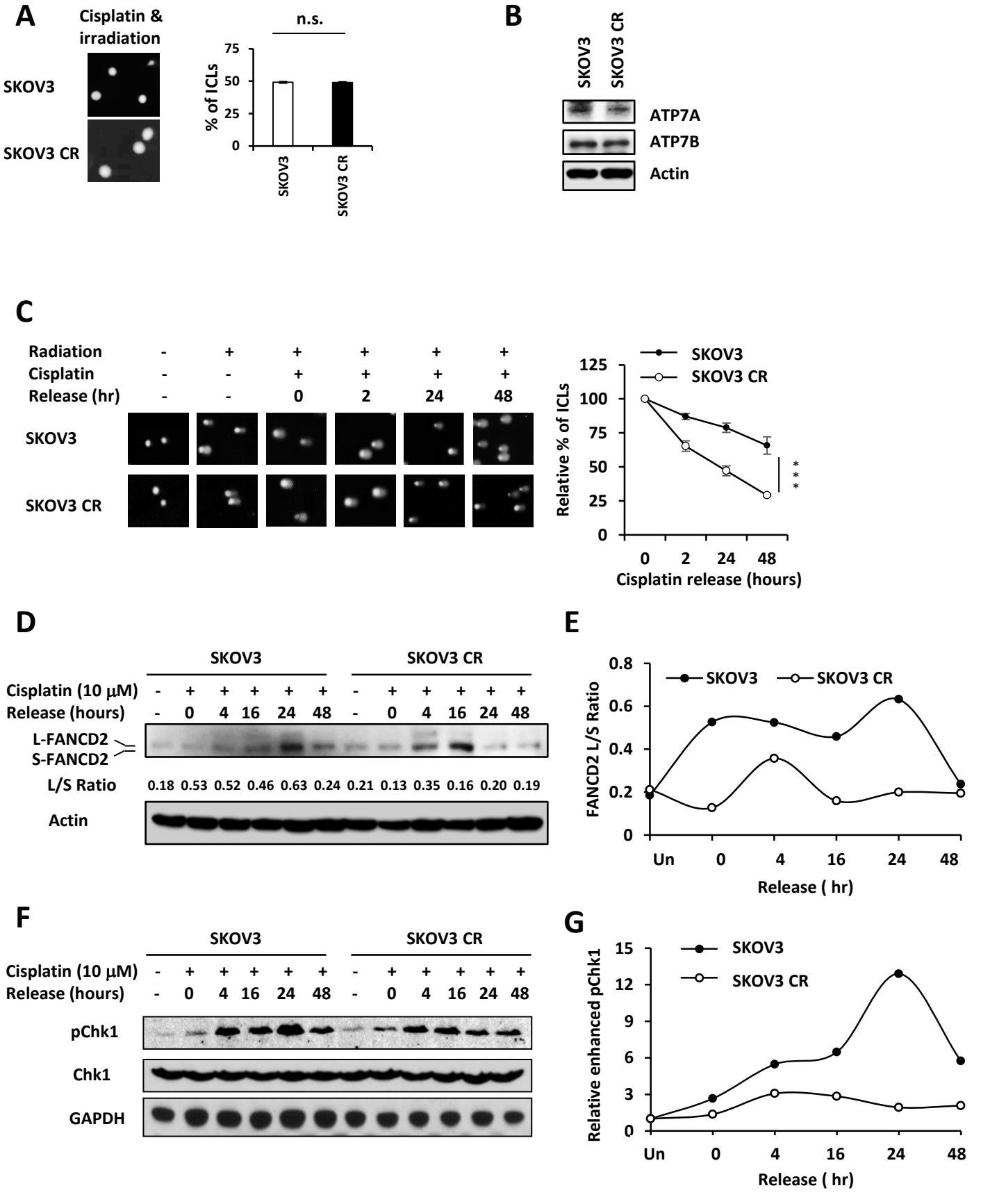
A
Cisplatin & irradiation
SKOV3
SKOV3 CR
n.s.
% of ICLs
75
50
25
0
SKOV3
SKOV3 CR
B
SKOV3
SKOV3 CR
ATP7A
ATP7B
Actin
C
Radiation - + + + + +
Cisplatin - - + + + +
Release (hr) - - 0 2 24 48
SKOV3
SKOV3 CR
SKOV3
SKOV3 CR
Relative % of ICLs
125
100
75
50
25
0
***
0 2 24 48
Cisplatin release (hours)
D
SKOV3
SKOV3 CR
Cisplatin (10 μM) - + + + + + - + + + + +
Release (hours) - 0 4 16 24 48 - 0 4 16 24 48
L-FANCD2
S-FANCD2
L/S Ratio 0.18 0.53 0.52 0.46 0.63 0.24 0.21 0.13 0.35 0.16 0.20 0.19
Actin
E
SKOV3
SKOV3 CR
FANCD2 L/S Ratio
0.8
0.6
0.4
0.2
0
Un 0 4 16 24 48
Release (hr)
F
SKOV3
SKOV3 CR
Cisplatin (10 μM) - + + + + + - + + + + +
Release (hours) - 0 4 16 24 48 - 0 4 16 24 48
pChk1
Chk1
GAPDH
G
SKOV3
SKOV3 CR
Relative enhanced pChk1
15
12
9
6
3
0
Un 0 4 16 24 48
Release (hr)

Figure 6

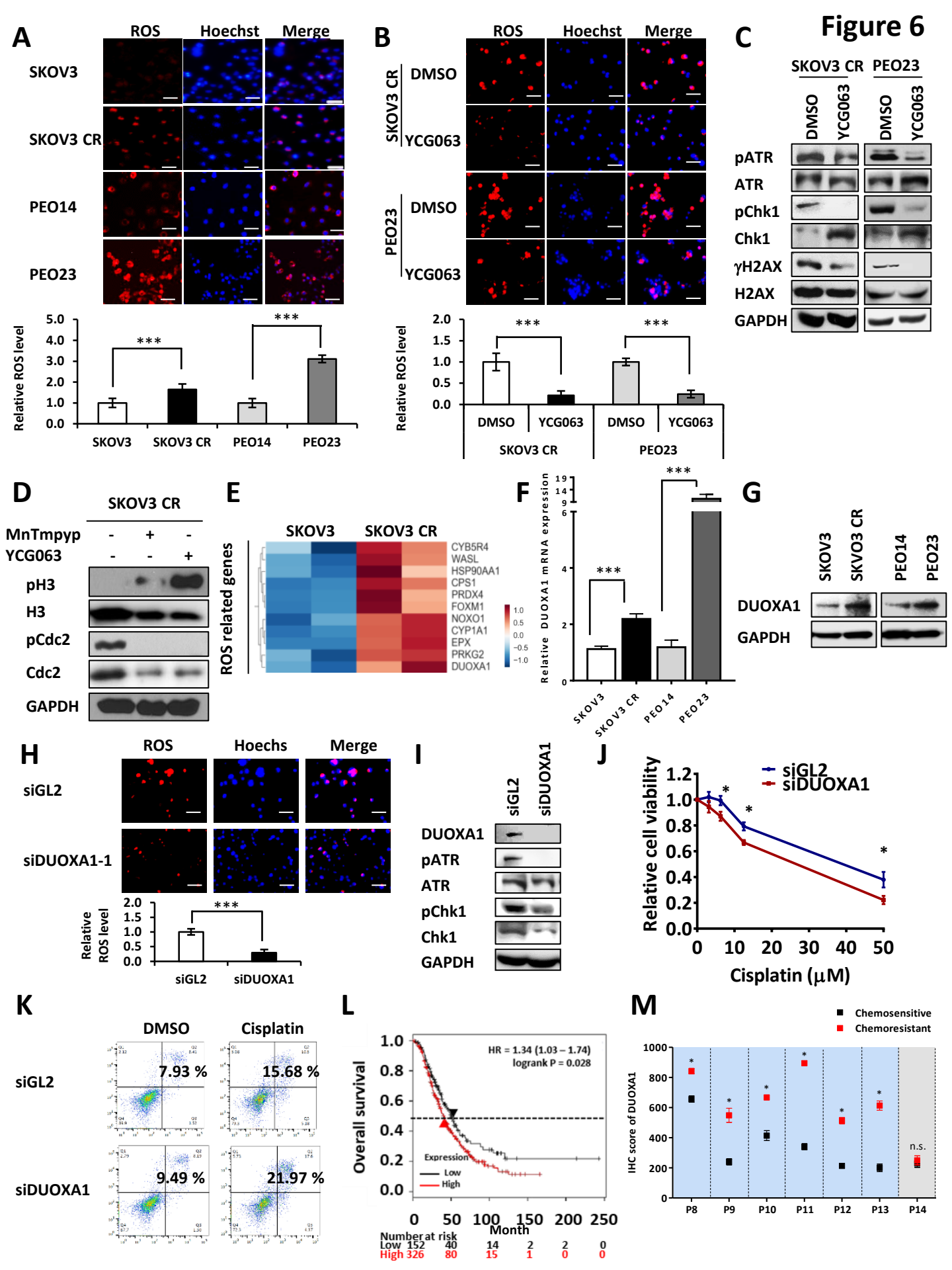
A
ROS
Hoechst
Merge
SKOV3
SKOV3 CR
PEO14
PEO23
Relative ROS level
SKOV3
SKOV3 CR
PEO14
PEO23
B
SKOV3 CR
DMSO
YCG063
PEO23
DMSO
YCG063
Relative ROS level
DMSO
YCG063
DMSO
YCG063
SKOV3 CR
PEO23
C
SKOV3 CR
PEO23
DMSO
YCG063
DMSO
YCG063
pATR
ATR
pChk1
Chk1
γH2AX
H2AX
GAPDH
D
SKOV3 CR
MnTmpyp
YCG063
pH3
H3
pCdc2
Cdc2
GAPDH
E
SKOV3
SKOV3 CR
ROS related genes
CYB5R4
WASL
HSP90AA1
CPS1
PRDX4
FOXM1
NOXO1
CYP1A1
EPX
PRKG2
DUOXA1
F
Relative DUOXA1 mRNA expression
SKOV3
SKOV3 CR
PEO14
PEO23
G
SKOV3
SKVO3 CR
PEO14
PEO23
DUOXA1
GAPDH
H
ROS
Hoechs
Merge
siGL2
siDUOXA1-1
Relative ROS level
siGL2
siDUOXA1
I
siGL2
siDUOXA1
DUOXA1
pATR
ATR
pChk1
Chk1
GAPDH
J
siGL2
siDUOXA1
Relative cell viability
Cisplatin (μM)
K
DMSO
Cisplatin
siGL2
7.93 %
15.68 %
siDUOXA1
9.49 %
21.97 %
L
HR = 1.34 (1.03 – 1.74)
logrank P = 0.028
Overall survival
Expression
Low
High
Month
Number at risk
Low 152 40 14 2 2 0
High 326 80 15 1 0 0
M
Chemosensitive
Chemoresistant
IHC score of DUOXA1
n.s.
P8
P9
P10
P11
P12
P13
P14

Figure 7

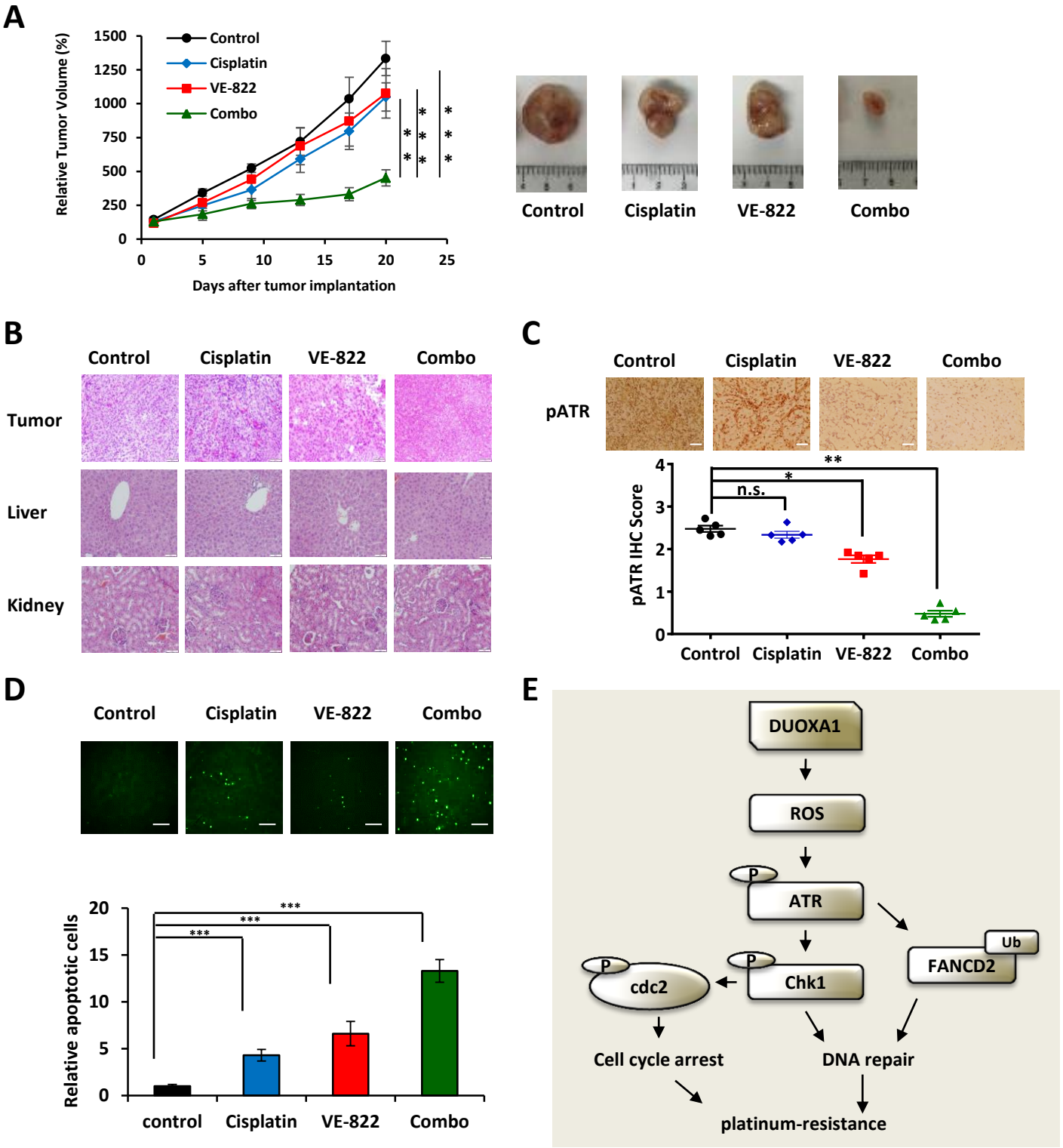
A
Relative Tumor Volume (%)
1500
1250
1000
750
500
250
0
0
5
10
15
20
25
Days after tumor implantation
Control
Cisplatin
VE-822
Combo
***
***
***
Control
Cisplatin
VE-822
Combo
B
Control
Cisplatin
VE-822
Combo
Tumor
Liver
Kidney
C
Control
Cisplatin
VE-822
Combo
pATR
pATR IHC Score
4
3
2
1
0
**
*
n.s.
Control
Cisplatin
VE-822
Combo
D
Control
Cisplatin
VE-822
Combo
Relative apoptotic cells
20
15
10
5
0
***
***
***
control
Cisplatin
VE-822
Combo
E
DUOXA1
ROS
P
ATR
P
Chk1
P
cdc2
Ub
FANCD2
Cell cycle arrest
DNA repair
platinum-resistance